IEEE Open Journal of Signal Processing

Received 3 January 2024; revised 8 March 2024; accepted 8 March 2024. Date of publication 13 March 2024;
date of current version 25 April 2024. The review of this article was arranged by Associate Editor Cihan Tepedelenlioglu.

*Digital Object Identifier 10.1109/OJSP.2024.3377098*

# Distributed Combined Channel Estimation and Optimal Uplink Receive Combining for User-Centric Cell-Free Massive MIMO Systems

**ROBBE VAN ROMPAEY (Member, IEEE) AND MARC MOONEN (Fellow, IEEE)**

Department of Electrical Engineering, KU Leuven, 3000 Leuven, Belgium

CORRESPONDING AUTHOR: ROBBE VAN ROMPAEY (e-mail: robbe.vanrompaey@esat.kuleuven.be).

The work of Robbe Van Rompaey was supported by the doctoral Fellowship of the Research Foundation Flanders (FWO-Vlaanderen). This work was supported in part by the ESAT Laboratory of KU Leuven, in the frame of FWO Research under Grant G0C0623 N "User-centric distributed signal processing algorithms for next generation cell-free massive MIMO based wireless communication networks" and in part by Fonds de la Recherche Scientifique—FNRS and Fonds Wetenschappelijk Onderzoek—Vlaanderen EOS under Grant 30452698 "(MUSE-WINET) MUlti-SErvice WIreless NETwork."

**ABSTRACT** Cell-free massive MIMO (CFmMIMO) is considered as one of the enablers to meet the demand for increasing data rates of next generation (6G) wireless communications. In user-centric CFmMIMO, each user equipment (UE) is served by a user-selected set of surrounding access points (APs), requiring efficient signal processing algorithms minimizing inter-AP communications, while still providing a good quality of service to all UEs. This paper provides algorithms for channel estimation (CE) and uplink (UL) receive combining (RC), designed for CFmMIMO channels using different assumptions on the structure of the channel covariances. Three different channel models are considered: line-of-sight (LoS) channels, non-LoS (NLoS) channels (the common Rayleigh fading model) and a combination of LoS and NLoS channels (the general Rician fading model). The LoS component introduces correlation between the channels at different APs that can be exploited to improve the CE and the RC. The channel estimates and receive combiners are obtained in each AP by processing the local antenna signals of the AP, together with compressed versions of all the other antenna signals of the APs serving the UE, during UL training. To make the proposed method scalable, the distributed user-centric channel estimation and receive combining (DUCERC) algorithm is presented that significantly reduces the necessary communications between the APs. The effectiveness of the proposed method and algorithm is demonstrated via numerical simulations.

**INDEX TERMS** Cell-free massive MIMO, CSI-free channel estimation, distributed user-centric processing, minimum-mean-squared-error (MMSE), uplink receive combining.

## I. INTRODUCTION

A major shortcoming of currently deployed cellular massive MIMO (mMIMO) networks (5G), where each user equipment (UE) is served only by the access point (AP) of the cell it resides in, is that UEs on cell edges experience a low channel gain to their serving AP and a high level of interference power from nearby cells [1]. To overcome this shortcoming, the concept of cell-free mMIMO (CFmMIMO) [2], [3], [4], [5], [6] has been proposed as a promising next step for next generation wireless communications (6G). Specifically, user-centric CFmMIMO [7], [8], [9], [10] is attracting a lot of attention, by letting the UEs themselves decide by which APs they are served [7], [11], [12]. Cooperation between the APs using the available fronthaul communication links then allows for implementing interference-rejecting receive combining (RC) and transmit precoding algorithms effective for all UEs in the network. Hence, CFmMIMO effectively eliminates cell borders while still reusing the current network layout, which offers the potential to drastically improve the user-experience as compared to current cellular mMIMO systems.

An important prerequisite for improving the user-experience, is obtaining good channel estimates of the channels between the UE and its serving APs. Currently. minimum-mean-squared-error (MMSE)-based channel

estimation (CE) [9], [13] using uplink (UL) pilots is seen as the standard, but requires perfect knowledge of the overall channel covariance, which is a rather strong assumption since the dimensions of the channel covariance grow with the number of antennas in the serving APs and furthermore the statistics are changing over time. Existing covariance estimators either require additional pilot transmission, sacrifice resources for data transmission [14], use strong assumptions on the distinguishability between channels that may not always be the case [15] or require knowledge of the pilot assignment of all the UEs in the network [16], [17]. Therefore, a new data-driven channel covariance estimator for low-rank channel covariances is proposed in [18], be it in the context of cellular mMIMO. It uses a generalized eigenvalue decomposition (GEVD) of two covariances that can be estimated from the available UL data. The requirements for the system are minimal and, except for synchronization, there is no need for communication between the different cells and no prior knowledge on the background noise is required. In this paper, this method is extended to CFmMIMO systems.

CE is mostly performed independently at each AP. While this is mostly justified for Rayleigh fading channels [2], [9], [13], i.e., channels with only non-line-of-sight (NLoS) components, due to the large spread in APs, this might no longer be the case for channels with an additional strong line-of-sight (LoS) component, i.e., satisfying the general Rician fading model. CFmMIMO systems with Rician fading channels are considered in [19], [20], [21], [22], without explicitly exploiting possible correlation between nearby APs serving common UEs. The data-driven channel covariance estimator allows for estimating correlation between nearby APs, and is thus able to exploit this to improve the CE and in a later stage the receive combining.

A low-complexity algorithm for local CE is presented in [23], requiring less resources to estimate the necessary channel state information (CSI). A time-of-arrival (TOA)-based scheme that first estimates the TOA of the multipath channel and then filters out interfering signals is presented in [24]. The TOA-based CE depends only on the currently received signal without the need for CSI. Both methods are compared to least-squares (LS) CE, but the estimation performance does not come close to MMSE-based CE. Methods based on machine learning [25], [26], [27] are arising and giving good estimation performance, especially for mmWave channels, since these channels can only approximately be described by Rayleigh and Rician fading models. While these methods reduce the online computational complexity, they require offline training and are tailored to particular setups.

UL RC [6], [28], [29] uses the acquired CSI to obtain a good estimate of the transmitted UL data. Popular UL RC choices in CFmMIMO are maximum-ratio (MR) combing [3], [8], [30], [31], local MMSE combining [13] and regularized zero-forcing [32], [33], [34]. In this paper, user-centric MMSE combining will be considered, requiring typically CSI of all antenna signals available in the user-centric network. It will be shown that optimal MMSE-based RC can efficiently be derived from the proposed CE by computing only a few additional parameters.

The newly presented CE and RC methods will first be derived in a centralized setting, i.e., as if all antenna signals serving a certain UE are gathered in one point of the network. As this requires a large communication bandwidth and furthermore introduces a single point of failure putting a heavy load on the backhaul network [35], a distributed algorithm will be presented, based on existing algorithms in wireless sensor networks [36], [37], [38], [39]. The channel estimates can then be obtained by processing the local antenna signals in each AP, together with compressed versions of all the other antenna signals of the APs serving the UE and computing a few extra parameters using in-network sums.

### A. NOVELTY

The contributions of the paper are summarized as follows:

- A randomized pilot assignment protocol for CFmMIMO systems is presented, allowing to estimate the channel covariance based on the observed UL data. Derivations of the corresponding optimal MMSE-based CE and RC are given for general channel covariances.
- Different data-based covariance estimation methods are proposed, based on different assumptions on the structure of the channel covariances, i.e., the channels contain only NLoS components (Rayleigh fading), only a LoS component, or contain both components (Rician fading). A GEVD-based procedure is used and closed-form expressions for GEVD-based CE and RC are presented.
- A distributed algorithm is derived to obtain the GEVD-based CE and RC in a scalable way, referred to as the GEVD-based distributed user-centric CE and RC (DUCERC) algorithm.
- Numerical simulations are provided for a simulated CFmMIMO system to evaluate the performance of the proposed centralized and distributed methods.

### B. PAPER OUTLINE

In Section II, the randomized pilot assignment protocol for CFmMIMO systems is presented. In Section III, different data-based covariance estimation methods are presented, based on different assumptions on the structure of the channel covariances. Also the GEVD-based procedure is explained and derived. In Section IV, the the distributed (DUCERC) algorithm is presented. The communication cost and convergence properties are also analysed. Furthermore, in Section V, it is explained how all channel estimates, available at each AP, can be used to improve the RC and can be included in the DUCERC algorithm. In Section VI, numerical simulations are provided.

### C. NOTATIONS

Bold lower case letters such as $\mathbf{a}$ are used to denote complex vectors, bold upper case letters such as $\mathbf{A}$ are used to denote complex matrices and the font $\mathbb{A}$ is used to denote submatrices, e.g., if $\mathbf{A} \in \mathbb{C}^{M \times N}$ then $\mathbb{A} \in \mathbb{C}^{P \times Q}$ corresponds

to a submatrix of $\mathbf{A}$ with $P \leq M$ and $Q \leq N$. $\mathbf{I}_R$ is the $R \times R$ identity matrix and $\mathbf{0}_{M\times N}$ is the all zero matrix of dimension $M \times N$. $|\cdot|, ||\cdot||_F, \cdot^H$ and $tr\{\cdot\}$ denote the absolute value, Frobenius norm, conjugate Hermitian operation and trace operation respectively. $E\{.\}$ is the expected value operator. $\lfloor\cdot\rfloor_0$ denotes $max(0,\cdot)$ and blkdiag$\{\mathbf{A}_1,\ldots,\mathbf{A}_K\}$ denotes a block diagonal matrix with $\mathbf{A}_1,\ldots,\mathbf{A}_K$ on its block diagonal. Finally $\mathcal{U}[a,b)$ denotes the uniform distribution in the interval $[a,b)$ and $\mathcal{NC}(\mathbf{a},\mathbf{A})$ is the complex Gaussian distribution with mean $\mathbf{a}$ and covariance $\mathbf{A}$. The overline notation $\overline{\cdot}$ will be used to denote true ('oracle') quantities, e.g. $\overline{\mathbf{R}}_k = E\{\mathbf{h}_k^t \mathbf{h}_k^{tH}\}$ will be used to denote the true channel covariance matrix where the expectations are defined with respect to all the different channel realizations. Symbols without overline will denote estimated quantities based on the available data by for example recursive time-averaging. Since this paper contains many symbols, an overview of the main symbols and their explanation is provided in Table 2 in the appendix section.

## II. CHANNEL AND SIGNAL MODEL

Consider a CFmMIMO network with $K$ single antenna UEs and $L$ APs, each having $N$ antennas[1] and local processing capabilities. Only a subset of the APs can observe the signal transmitted by UE $k$ with a non-zero SINR. It is often enough to only include APs that observe the signal transmitted by UE $k$ with a significant SINR and consider the signal transmitted by UE $k$ as noise at the other APs. This subset will be denoted as

$$\mathcal{M}_k = \{l | \text{AP } l \text{ observes UE } k\} = \{1,\ldots,L_k\} \tag{1}$$

where $\{1,\ldots,L_k\}$ defines a specific ordering of the APs for UE $k$.

The local antenna signal $\mathbf{y}_l$ of AP $l$ can be written as[2]

$$\mathbf{y}_l^t = \sum_{k\in\mathcal{D}_l} \mathbf{h}_{kl}^t s_k + \mathbf{n}_l^t \in \mathbb{C}^N \tag{2}$$

where $\mathbf{h}_{kl}^t$ is the channel between UE $k$ and AP $l$ which can be assumed fixed in one coherence block $t$ of $\tau$ samples [7], $\mathbf{n}_l^t$ is an additive noise component with covariance $\overline{\mathbf{R}}_{\mathbf{n}_l\mathbf{n}_l} = E\{\mathbf{n}_l^t \mathbf{n}_l^{tH}\}$ and $s_k$ is the signal transmitted by UE $k$, assumed to have unit transmit power. When UE $k$ is using a transmit power $p_k$ different from unity, the channel can be redefined as the virtual channel $\mathbf{h}_{kl}^t\sqrt{p_k}$, such that again the transmit power becomes one.[3] This simplification is used throughout the paper to avoid overly complicated formulas. Finally, the set

$$\mathcal{D}_l = \{k | l \in \mathcal{M}_k\} \tag{3}$$

is the set of UEs that AP $l$ observes.

To make the setup scalable, only the antenna signals of the APs in $\mathcal{M}_k$ will be used to estimate $s_k$. Therefore, a user-centric (sub-)network $\mathcal{M}_k$ will be formed to serve UE $k$ as depicted in Fig. 1 and their antenna signals are gathered in the (combined) user-centric antenna signal $\mathbf{y}^{\mathcal{M}_k t}$ as

$$\mathbf{y}^{\mathcal{M}_k t} = \mathbf{h}_k^{\mathcal{M}_k t} s_k + \sum_{\tilde{k}\in\tilde{\mathcal{P}}_k} \mathbf{h}_{\tilde{k}}^{\mathcal{M}_k t} s_{\tilde{k}} + \mathbf{n}^{\mathcal{M}_k t} \in \mathbb{C}^{NL_k} \tag{4}$$

where $\mathbf{y}^{\mathcal{M}_k t} = [\mathbf{y}_1^{tH} \ \ldots \ \mathbf{y}_{L_k}^{tH}]^H$, $\mathbf{h}_k^{\mathcal{M}_k t} = [\mathbf{h}_{k1}^{tH} \ \ldots \ \mathbf{h}_{kL_k}^{tH}]^H$ and $\mathbf{n}^{\mathcal{M}_k t} = [\mathbf{n}_1^{tH} \ \ldots \ \mathbf{n}_{L_k}^{tH}]^H$. Note that $\mathbf{h}_k^t$ is shorthand notation for $\mathbf{h}_k^{\mathcal{M}_k t}$ and both notations will be used. Also $\mathbf{h}_{\tilde{k}}^{\mathcal{M}_k t}$ contains the channels from UE $\tilde{k}$ to the APs in $\mathcal{M}_k$. This can be written as $\mathbf{E}_{\tilde{k}}^{\mathcal{M}_k}\mathbf{h}_{\tilde{k}}^t$ where $\mathbf{E}_{\tilde{k}}^{\mathcal{M}_k} \in \mathbb{C}^{NL_k\times NL_{\tilde{k}}}$ is a selection matrix that selects the channels $\mathbf{h}_{\tilde{k}l}^t$ in $\mathbf{h}_{\tilde{k}}^t$ if AP $l \in \mathcal{M}_k$ and inserts zero channels elsewhere. It is further assumed that the noise is uncorrelated between the APs, so $\overline{\mathbf{R}}_{\mathbf{nn}}^{\mathcal{M}_k} = \text{blkdiag}\{\overline{\mathbf{R}}_{\mathbf{n}_1\mathbf{n}_1},\ldots,\overline{\mathbf{R}}_{\mathbf{n}_{L_k}\mathbf{n}_{L_k}}\}$. Finally

$$\mathcal{P}_k = \{\tilde{k} | \mathcal{M}_{\tilde{k}} \cap \mathcal{M}_k \neq \emptyset\} = \{1,\ldots,K_k\} \tag{5}$$

is the set of UEs that cause interference in the antenna signals $\mathbf{y}^{\mathcal{M}_k t}$ where $\{1,\ldots,K_k\}$ denotes a specific ordering of the UEs for UE $k$ and $\tilde{\mathcal{P}}_k \triangleq \mathcal{P}_k \setminus \{k\}$.

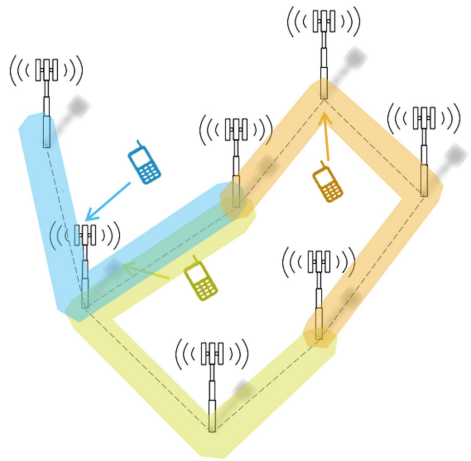

**FIGURE 1.** Network with user-centric (sub)-networks in which the signal of a UE is processed.

### A. CHANNEL MODEL

The channel $\mathbf{h}_k^t$ is assumed to remain constant during one coherence block and is typically modeled as being drawn from an independent correlated Rician fading distribution [19]:

$$\mathbf{h}_k^t = \underline{\mathbf{h}}_k e^{j\varphi_k^t} + \mathbf{g}_k^t \tag{6}$$

with $\varphi_k^t \sim \mathcal{U}[0,2\pi)$ and $\mathbf{g}_k^t \sim \mathcal{NC}(\mathbf{0},\overline{\mathbf{G}}_k)$ in each coherence block. Here, $\underline{\mathbf{h}}_k$ is the LoS component, $e^{j\varphi_k^t}$ is a random

[1] The methods and algorithms proposed in this paper can easily be extended to scenarios where different APs have a different number of antennas (for ease of notation the same number of antennas are assumed throughout the paper).

[2] Note that abstraction is made of the practical Orthogonal Frequency Division Multiplexing (OFDM) based multi-carrier modulation. [40, Sec. 2] explains how this simplification can be derived.

[3] In general, the transmitted power during the uplink training phase and the uplink data transmission phase can be different and optimized separately. However, for ease of exposition, they are assumed to be the same in this paper. The reader can easily extend the formulas by adding power factors to all channel-related parameters.

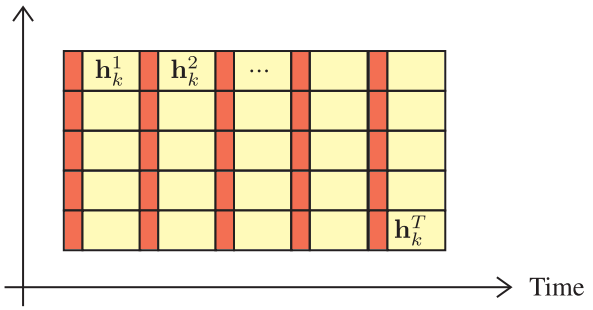


**FIGURE 2. Time-frequency resources shared during transmission with division in samples for CE (red) and UL data transmission (yellow). Although the channels $\{\mathbf{h}_k^1, \ldots, \mathbf{h}_k^T\}$ are different in each coherence block, they are assumed to be generated by the same large-scale fading statistics (e.g. $\underline{\overline{\mathbf{h}}}_k$ and $\overline{\mathbf{G}}_k$) that remain constant for several coherence blocks.**

phase shift and $\overline{\mathbf{G}}_k \in \mathbb{C}^{NL_k \times NL_k}$ is the positive (semi-)definite spatial channel covariance describing the large-scale fading, including geometric pathloss, shadowing, antenna gains and spatial channel correlation [41]. The uniform and Gaussian distribution model the small-scale fading of the Los and NLoS component respectively. The LoS component and large-scale fading are assumed to remain constant over several thousands of coherence blocks as indicated by Fig. 2. Further note that

$$E\{\mathbf{h}_k^t\} = \mathbf{0}_{NL_k} \text{ and } E\{\mathbf{h}_k^t \mathbf{h}_k^{tH}\} = \underline{\overline{\mathbf{h}}}_k \underline{\overline{\mathbf{h}}}_k^H + \overline{\mathbf{G}}_k \triangleq \overline{\mathbf{R}}_k. \tag{7}$$

It is common in the CFmMIMO literature to assume that the channels between a UE and different APs are independently distributed, i.e., $E\{\mathbf{h}_{kl}^t \mathbf{h}_{k\tilde{l}}^{tH}\} = \mathbf{0}_{N\times N}$ for $l \neq \tilde{l}$, so that $\overline{\mathbf{R}}_k$ in (7) is block diagonal and that CE can be performed independently at each AP, based on $\overline{\mathbf{R}}_{kl}$, denoting the $l$th diagonal block of $\overline{\mathbf{R}}_k$. This assumption might be motivated by the large spatial distribution of the APs in the network. While this is valid for the NLoS component, the assumption is no longer valid for the LoS component $\underline{\overline{\mathbf{h}}}_k$, since user-centric processing is considered here and only APs in the neighborhood of UE $k$ are serving UE $k$, Therefore, it is possible to have correlation between the APs, represented by non-zero non-diagonal blocks in $\overline{\mathbf{R}}_k$. This will have a significant impact on the execution of the CE.

It is further assumed that channels from different UEs are uncorrelated $E\{\mathbf{h}_k^t \mathbf{h}_{\tilde{k}}^{tH}\} = \mathbf{0}_{NL_k \times NL_{\tilde{k}}}$.

### B. CHANNEL ESTIMATION

The samples in one coherence block will be divided into $\tau_p$ samples for CE and $\tau_u$ samples for UL data transmission, indicated in red and yellow respectively in Fig. 2. The CE procedure from [18] will be adopted here, which is summarized as follows. The $\tau_p$ reserved samples can be used to define $\tau_p$ orthogonal pilot sequences and each UE can randomly select one of these pilot sequences in each coherence block. It is also assumed that APs know which pilot sequences are selected by the UEs that they serve, which can for example be accomplished using pseudo-random generators with the same seed. The received antenna signals at the APs can then be despread[4] using the $\tau_p$ different pilot sequences, denoted by $\mathbf{y}_{all_k}^{\mathcal{M}_k t}[p]$ where $p = 1, \ldots, \tau_p$ is the index of the pilot sequence. The signal obtained after despreading with the correct pilot sequence $\tau_k$ for UE $k$ is denoted by $\mathbf{y}_{\tau_k}^{\mathcal{M}_k t}$. As shown in [18], these signals can be written as

$$\mathbf{y}_{\tau_k}^{\mathcal{M}_k t} = \sqrt{\tau_p}\mathbf{h}_k^t + \sqrt{\tau_p} \sum_{\tilde{k}\in\tilde{\mathcal{P}}_k} \mathbf{h}_{\tilde{k}}^{\mathcal{M}_k t} \delta_{\tilde{k}} + \mathbf{n}^{\mathcal{M}_k t} \tag{8}$$

$$\mathbf{y}_{all_k}^{\mathcal{M}_k t}[p] = \sqrt{\tau_p}\mathbf{h}_k^t \delta_k + \sqrt{\tau_p} \sum_{\tilde{k}\in\tilde{\mathcal{P}}_k} \mathbf{h}_{\tilde{k}}^{\mathcal{M}_k t} \delta_{\tilde{k}} + \mathbf{n}^{\mathcal{M}_k t} \tag{9}$$

where $\delta_{\tilde{k}}$ is a random variable with $E\{\delta_{\tilde{k}}\} = \frac{1}{\tau_p}$ and $E\{\delta_{\tilde{k}}^2\} = \frac{1}{\tau_p}$. It models the probability that a UE choses a given pilot sequence in one coherence block. The additive noise $\mathbf{n}^{\mathcal{M}_k t}$ has still the same covariance $\overline{\mathbf{R}}_{\mathbf{nn}}^{\mathcal{M}_k}$ as the noise in (4) as proven in [18]. The factor $\sqrt{\tau_p}$ is an extra gain factor emerging from the despreading procedure.

Expressions for the covariances of the signals in (8) and (9) are also derived in [18] as

$$\overline{\mathbf{R}}_{\tau_k}^{\mathcal{M}_k} = E\left\{\mathbf{y}_{\tau_k}^{\mathcal{M}_k t} \mathbf{y}_{\tau_k}^{\mathcal{M}_k t^H}\right\} = \tau_p \overline{\mathbf{R}}_k + \sum_{\tilde{k}\in\tilde{\mathcal{P}}_k} \overline{\mathbf{R}}_{\tilde{k}}^{\mathcal{M}_k} + \overline{\mathbf{R}}_{\mathbf{nn}}^{\mathcal{M}_k}$$

$$\overline{\mathbf{R}}_{all_k}^{\mathcal{M}_k} = E\left\{\frac{1}{\tau_p}\sum_{p=1}^{\tau_p} \mathbf{y}_{all_k}^{\mathcal{M}_k t}[p] \mathbf{y}_{all_k}^{\mathcal{M}_k t^H}[p]\right\} = \overline{\mathbf{R}}_k + \sum_{\tilde{k}\in\tilde{\mathcal{P}}_k} \overline{\mathbf{R}}_{\tilde{k}}^{\mathcal{M}_k} + \overline{\mathbf{R}}_{\mathbf{nn}}^{\mathcal{M}_k} \tag{10}$$

where $\overline{\mathbf{R}}_{\tilde{k}}^{\mathcal{M}_k}$ is defined as $\mathbf{E}_{\tilde{k}}^{\mathcal{M}_k} \overline{\mathbf{R}}_{\tilde{k}} \mathbf{E}_{\tilde{k}}^{\mathcal{M}_k H}$ and $\overline{\mathbf{R}}_k$ as defined in (7) is shorthand notation for $\overline{\mathbf{R}}_k^{\mathcal{M}_k}$. Similarly $\overline{\mathbf{R}}_{\tau_k}$ and $\overline{\mathbf{R}}_{all_k}$ will be used as shorthand notation for $\overline{\mathbf{R}}_{\tau_k}^{\mathcal{M}_k}$ and $\overline{\mathbf{R}}_{all_k}^{\mathcal{M}_k}$ respectively.

With these covariances an expression can be derived for the (unknown) channel covariance

$$\Rightarrow \overline{\mathbf{R}}_k = \frac{1}{\tau_p - 1}\left(\overline{\mathbf{R}}_{\tau_k} - \overline{\mathbf{R}}_{all_k}\right) \tag{11}$$

which will be used to compute a CE filter.

In practice $\overline{\mathbf{R}}_{\tau_k}$ and $\overline{\mathbf{R}}_{all_k}$ will be estimated from the data using a moving average filter (note that the overline-notation for $\overline{\mathbf{R}}_{\tau_k}$ is now removed), e.g.,

$$\mathbf{R}_{\tau_k}(t) = \frac{1}{T}\sum_{\tilde{t}=t-T+1}^{t} \mathbf{y}_{\tau_k}^{\mathcal{M}_k \tilde{t}} \mathbf{y}_{\tau_k}^{\mathcal{M}_k \tilde{t}^H} \tag{12}$$

or a recursive averaging filter:

$$\mathbf{R}_{\tau_k}(t) = (1-\lambda)\mathbf{R}_{\tau_k}(t-1) + \lambda \mathbf{y}_{\tau_k}^{\mathcal{M}_k t} \mathbf{y}_{\tau_k}^{\mathcal{M}_k t^H}. \tag{13}$$

However, directly using (11) with the estimated covariances $\mathbf{R}_{\tau_k}$ and $\mathbf{R}_{all_k}$, will not result in a good estimate for $\mathbf{R}_k$ [18]: it may result in an estimate that is not positive (semi-)definite

[4] i.e. multiplied with complex conjugate of a pilot sequence.

and/or antenna signals with a poor signal-to-noise ratio may strongly influence the estimation. Therefore, based on different assumptions on the structure of $\overline{\mathbf{R}}_k$, different estimation methods will be provided in Section III to overcome this issue.

The optimal MMSE-based CE filter is then obtained by minimizing an MMSE criterion [19]

$$\overline{\mathbf{W}}_k = \arg\min_{\boldsymbol{W}_k} E\{||\mathbf{h}_k^t - \boldsymbol{W}_k^H \mathbf{y}_{\tau_k}^{\mathcal{M}_k t}||^2\} = \sqrt{\tau_p}(\overline{\mathbf{R}}_{\tau_k})^{-1}\overline{\mathbf{R}}_k \tag{14}$$

since $E\{\mathbf{y}_{\tau_k}^{\mathcal{M}_k t}\mathbf{h}_k^{t^H}\} = \sqrt{\tau_p}\overline{\mathbf{R}}_k$. This results in an unbiased estimate $\mathbf{h}_k^t \sim \mathcal{NC}(\hat{\overline{\mathbf{h}}}_k^t, \overline{\mathbf{C}}_k)$ with

$$\begin{aligned}\hat{\overline{\mathbf{h}}}_k^t &= \overline{\mathbf{W}}_k^H \mathbf{y}_{\tau_k}^{\mathcal{M}_k t} \\ \overline{\mathbf{C}}_k &= E\left\{(\hat{\overline{\mathbf{h}}}_k^t - \mathbf{h}_k^t)(\hat{\overline{\mathbf{h}}}_k^t - \mathbf{h}_k^t)^H\right\} = \overline{\mathbf{R}}_k - \sqrt{\tau_p}\overline{\mathbf{R}}_k\overline{\mathbf{W}}_k.\end{aligned} \tag{15}$$

Note that when $\overline{\mathbf{R}}_{\tau_k}^{\mathcal{M}_k}$ and $\overline{\mathbf{R}}_k$ are not block diagonal, $\overline{\mathbf{W}}_k$ will generally not be a block diagonal matrix either. Therefore, all signals in $\mathbf{y}_{\tau_k}^{\mathcal{M}_k t}$ will be used to compute an estimate $\hat{\overline{\mathbf{h}}}_{kl}^t$ of the channel between UE $k$ and AP $l$, not only the local signals $\mathbf{y}_{\tau_k l}^t$ available at AP $l$. Efficient distributed algorithms will be provided in Section III to prevent that all these signals have to be gathered at some point in the network, while still obtaining the correct local channel estimate.

### C. RECEIVE COMBINING

The next $\tau_u$ samples will be used by UE $k$ for UL data transmission. The data signal $s_k$ will be estimated in the user-centric network $\mathcal{M}_k$ by linearly combining the antenna signals in (4) with a receive combiner $\mathbf{v}_k^t \in \mathbb{C}^{NL_k}$ derived from the acquired channel estimates. This linear combining can be performed in the user-centric network if each AP in $\mathcal{M}_k$ selects the local receive combiner $\mathbf{v}_{kl}^t \in \mathbb{C}^N$ in $\mathbf{v}_k^t = [\mathbf{v}_{k1}^{t^H} \ \ldots \ \mathbf{v}_{kL_k}^{t^H}]^H$ and computes the local estimate as $\hat{s}_{kl} = \mathbf{v}_{kl}^{t^H}\mathbf{y}_l^t$. If the APs in $\mathcal{M}_k$ are organized in a connected topology (as will be discussed in Section IV), they can compute an in-network sum to obtain the final estimate as $\hat{s}_k = \sum_{l\in\mathcal{M}_k}\hat{s}_{kl} = \mathbf{v}_k^{t^H}\mathbf{y}_k^{\mathcal{M}_k t}$.

MMSE-based RC will be considered here. The MMSE-based receive combiner $\overline{\mathbf{v}}_k^t$, which only uses the acquired channel estimates of UE $k$, is given as

$$\begin{aligned}\overline{\mathbf{v}}_k^t &= \arg\min_{\boldsymbol{v}_k} E\{|s_k - \boldsymbol{v}_k^H \mathbf{y}^{\mathcal{M}_k t}|^2 \Big| \mathbf{h}_k^t \sim \mathcal{NC}(\hat{\overline{\mathbf{h}}}_k^t, \overline{\mathbf{C}}_k)\} \\ &= \left(\sum_{\tilde{k}\in\tilde{\mathcal{P}}_k} \overline{\mathbf{R}}_{\tilde{k}}^{\mathcal{M}_k} + \overline{\mathbf{R}}_{\mathbf{nn}}^{\mathcal{M}_k} + \overline{\mathbf{C}}_k + \hat{\overline{\mathbf{h}}}_k^t \hat{\overline{\mathbf{h}}}_k^{t^H}\right)^{-1} \hat{\overline{\mathbf{h}}}_k^t \\ &= \left(\overline{\mathbf{R}}_{\tau_k}^{\mathcal{M}_k} - \tau_p\overline{\mathbf{R}}_k + \overline{\mathbf{C}}_k + \hat{\overline{\mathbf{h}}}_k^t \hat{\overline{\mathbf{h}}}_k^{t^H}\right)^{-1} \hat{\overline{\mathbf{h}}}_k^t\end{aligned} \tag{16}$$

where the fact that

$$\begin{aligned}&E\left\{\mathbf{y}^{\mathcal{M}_k t}\mathbf{y}^{\mathcal{M}_k t^H} \Big| \mathbf{h}_k^t \sim \mathcal{NC}(\hat{\overline{\mathbf{h}}}_k^t, \overline{\mathbf{C}}_k)\right\} = \\ &\sum_{\tilde{k}\in\tilde{\mathcal{P}}_k} E\left\{\mathbf{h}_{\tilde{k}}^{\mathcal{M}_k t}\mathbf{h}_{\tilde{k}}^{\mathcal{M}_k t^H}\right\} + E\left\{\mathbf{n}^{\mathcal{M}_k t}\mathbf{n}^{\mathcal{M}_k t^H}\right\} + E\left\{\mathbf{h}_k^t\mathbf{h}_k^{t^H}|\mathbf{h}_k^t\right\}\end{aligned} \tag{17}$$

is used in the second step of (16). This receive combiner only requires knowledge of the channel estimate of UE $k$ whereas the interference/noise will be canceled based on their presence in $\overline{\mathbf{R}}_{\tau_k}^{\mathcal{M}_k}$.

A different MMSE-based receive combiner can also be constructed when channel estimates of all the other UEs in $\mathcal{P}_k$ are available, which will be referred to as multi-user RC and will be considered in Section V. The expression for this receive combiner $\overline{\mathbf{w}}_k^t$ is given as

$$\begin{aligned}\overline{\mathbf{w}}_k^t &= \arg\min_{\boldsymbol{w}_k} E\left\{|s_k - \boldsymbol{w}_k^H \mathbf{y}^{\mathcal{M}_k t}|^2 \Big| \right. \\ &\qquad \left. \{\mathbf{h}_{\tilde{k}}^{\mathcal{M}_k t} \sim \mathcal{NC}(\hat{\overline{\mathbf{h}}}_{\tilde{k}}^{\mathcal{M}_k t}, \overline{\mathbf{C}}_{\tilde{k}}^{\mathcal{M}_k})\}_{\forall \tilde{k}\in\mathcal{P}_k}\right\} \\ &= \left(\overline{\mathbf{R}}_{\mathbf{nn}}^{\mathcal{M}_k} + \sum_{\tilde{k}\in\mathcal{P}_k} (\overline{\mathbf{C}}_{\tilde{k}}^{\mathcal{M}_k} + \hat{\overline{\mathbf{h}}}_{\tilde{k}}^{\mathcal{M}_k t}\hat{\overline{\mathbf{h}}}_{\tilde{k}}^{\mathcal{M}_k t^H})\right)^{-1} \hat{\overline{\mathbf{h}}}_k^t \\ &= \left(\overline{\mathbf{R}}_{all_k} + \sum_{\tilde{k}\in\mathcal{P}_k} (\overline{\mathbf{C}}_{\tilde{k}}^{\mathcal{M}_k} - \overline{\mathbf{R}}_{\tilde{k}}^{\mathcal{M}_k} + \hat{\overline{\mathbf{h}}}_{\tilde{k}}^{\mathcal{M}_k t}\hat{\overline{\mathbf{h}}}_{\tilde{k}}^{\mathcal{M}_k t^H})\right)^{-1} \hat{\overline{\mathbf{h}}}_k^t\end{aligned} \tag{18}$$

where $\overline{\mathbf{C}}_{\tilde{k}}^{\mathcal{M}_k}$ is defined as $\mathbf{E}_{\tilde{k}}^{\mathcal{M}_k}\overline{\mathbf{C}}_{\tilde{k}}\mathbf{E}_{\tilde{k}}^{\mathcal{M}_k H}$.

The expressions for the receive combiner filters $\mathbf{v}_k^t$ and $\mathbf{w}_k^t$ show that user-centric CSI is required, so this can again only be accomplished when all the user-centric antenna signals in $\mathbf{y}^{\mathcal{M}_k t}$ are available. In the next section, expressions for the channel estimates and receive combiners will be derived depending on the assumed channel model of $\overline{\mathbf{R}}_k$ and assuming that all user-centric antenna signals are centralized at some point in the user-centric network $\mathcal{M}_k$. It will become clear that the expressions allow for efficient distributed processing, which will be further elaborated upon in Section IV.

## III. CENTRALIZED GEVD-BASED CE AND RC

Performing the subtraction as in (11) using estimated covariances $\mathbf{R}_{\tau_k}$ and $\mathbf{R}_{all_k}$ and without taking into account possible knowledge on the structure of $\overline{\mathbf{R}}_k$, has significant drawbacks [18]. Therefore, it is proposed to estimate $\mathbf{R}_k$ by minimizing the following objective [42]

$$\mathbf{R}_k = \arg\min_{\boldsymbol{R}_k} \|\mathbf{R}_{\tau_k}^{-1/2}\left(\mathbf{R}_{\tau_k} - \mathbf{R}_{all_k} - (\tau_p - 1)\boldsymbol{R}_k\right)\mathbf{R}_{\tau_k}^{-H/2}\|_F^2 \tag{19}$$

with some constraints on the structure of $\boldsymbol{R}_k$ (a default constraint is that $\mathbf{R}_k$ should be positive semi-definite). Rather than using an unweighted Frobenius norm, where absolute

(squared) approximation errors are summed in the matrix approximation problem (19), it is more appropriate to consider relative approximation errors, where larger errors are tolerated in places where there is a lot of noise/interference, which are represented by large values in $\mathbf{R}_{\tau_k}$. This is done by including a prewhitening operation with $\mathbf{R}_{\tau_k}^{-1/2}$ and $\mathbf{R}_{\tau_k}^{-H/2}$.

In this section, three different channel models are considered and closed-form expressions for the channel estimate and receive combiner $\mathbf{v}_k^t$ are derived. Closed-form expressions for receive combiner $\mathbf{w}_k^t$ will be derived in Section V. The channel models are: (i) block diagonal $\overline{\mathbf{R}}_k$ with a local rank constraint, (ii) low rank $\overline{\mathbf{R}}_k$ with a user-centric rank constraint and (iii) a combination of (i) and (ii).

### A. BLOCK DIAGONAL $\overline{\mathbf{R}}_k$ WITH LOCAL RANK $R^B$

In this subsection, a block diagonal $\overline{\mathbf{R}}_k$ will be considered, where only the diagonal blocks $\overline{\mathbf{R}}_{kl}$ for $l \in \mathcal{M}_k$ are non-zero. This is the most commonly assumed model in CFmMIMO literature [8], since the LoS-component in (6) is often neglected in rich scattering scenarios. When the channel is seen as a superposition of multipath components, coming from an area localized around the UE, this often results in a low rank channel covariance $\overline{\mathbf{R}}_{kl}$ [17], [41]. Simulations in [18] show that a rank $R^B$ equal to $N/2$ gives a good performance for these channel models.

Therefore, the following structure is imposed on $\overline{\mathbf{R}}_k$

$$\overline{\mathbf{R}}_k = \overline{\mathbf{Q}}_k^B \overline{\mathbf{\Sigma}}_k^B \overline{\mathbf{Q}}_k^{B^H} \tag{20}$$

with $\overline{\mathbf{Q}}_k^B$ and $\overline{\mathbf{\Sigma}}_k^B$ defined as

$$\begin{aligned} \overline{\mathbf{Q}}_k^B &= \text{blkdiag}\{\overline{\mathbb{Q}}_{k1}^B, \ldots, \overline{\mathbb{Q}}_{kL_k}^B\} \\ \overline{\mathbf{\Sigma}}_k^B &= \text{blkdiag}\{\overline{\mathbb{\Sigma}}_{k1}^B, \ldots, \overline{\mathbb{\Sigma}}_{kL_k}^B\} \end{aligned} \tag{21}$$

and with $\overline{\mathbb{Q}}_{kl}^B \in \mathbb{C}^{N \times R^B}$ and $\overline{\mathbb{\Sigma}}_{kl}^B \in \mathbb{C}^{R^B \times R^B}$.

Since $\overline{\mathbf{R}}_{\tau_k}$, $(\overline{\mathbf{R}}_{\tau_k})^{-1}$ and $\overline{\mathbf{R}}_{all_k}$ are then also block diagonal, (19) can be decomposed in $L_k$ subproblems that can be solved seperately and optimally using $L_k$ GEVDs of matrix pencils $\{\mathbf{R}_{\tau_k l}, \mathbf{R}_{all_k l}\}$ [42]:

$$\begin{aligned} \mathbf{R}_{\tau_k l} &= \mathbf{Q}_{kl}^B \mathbf{Q}_{kl}^{B^H} \\ \mathbf{R}_{all_k l} &= \mathbf{Q}_{kl}^B \mathbf{\Sigma}_{all_k l}^B \mathbf{Q}_{kl}^{B^H}. \end{aligned} \tag{22}$$

Here $\mathbf{Q}_{kl}^B \in \mathbb{C}^{N \times N}$ is an invertible matrix, its Hermitian inverse contains the generalized eigenvectors as columns, and $\mathbf{\Sigma}_{all_k l}^B \in \mathbb{C}^{N \times N}$ is a diagonal matrix containing the inverse of the generalized eigenvalues, where the diagonal elements are sorted from small to large. Let $\mathbb{\Sigma}_{all_k,l}^B$ denote the $R^B \times R^B$ diagonal matrix with the first $R^B$ columns and rows of $\mathbf{\Sigma}_{all_k l}^B$. The optimal solution for $\mathbf{R}_{kl}$ in (19) is then given by [42]

$$\mathbf{R}_{kl} = \mathbb{Q}_{kl}^B \mathbb{\Sigma}_{kl}^B \mathbb{Q}_{kl}^{B^H} \tag{23}$$

where

$$\begin{aligned} \mathbb{\Sigma}_{kl}^B &= \frac{1}{\tau_p - 1} \lfloor \mathbf{I}_{R^B} - \mathbb{\Sigma}_{all_k l}^B \rfloor_0 \\ \mathbb{Q}_{kl}^B &= \mathbf{Q}_{kl}^B [\mathbf{I}_{R^B} \ \mathbf{0}_{R^B \times (N - R^B)}]^H. \end{aligned} \tag{24}$$

Also define

$$\mathbb{X}_{kl}^B = \left(\mathbf{Q}_{kl}^B\right)^{-H} [\mathbf{I}_{R^B} \ \mathbf{0}_{R^B \times (N - R^B)}]^H = \mathbf{R}_{\tau_k l}^{-1} \mathbb{Q}_{kl}^B \tag{25}$$

such that $\mathbb{X}_{kl}^{B^H} \mathbb{Q}_{kl}^B = \mathbf{I}_{R^B}$. An estimate of the full channel covariance (23) is then obtained by replacing time quantities in (21) by the estimated quantities from (24).

The MMSE-based CE filter $\mathbf{W}_k$ with the estimated quantities and the estimated $\mathbf{R}_k$ is then also block diagonal with $l$th block diagonal

$$\mathbf{W}_{kl} = \sqrt{\tau_p} \mathbf{R}_{\tau_k l}^{-1} \mathbf{R}_{kl} = \sqrt{\tau_p} \mathbb{X}_{kl}^B \mathbb{\Sigma}_{kl}^B \mathbb{Q}_{kl}^{B^H}. \tag{26}$$

The corresponding channel estimates and estimation error covariance are given by

$$\begin{aligned} \hat{\mathbf{h}}_{kl}^t &= \mathbf{W}_{kl}^H \mathbf{y}_{\tau_k l}^t = \mathbb{Q}_{kl}^B \underbrace{\sqrt{\tau_p} \mathbb{\Sigma}_{kl}^B \mathbb{X}_{kl}^{B^H} \mathbf{y}_{\tau_k l}^t}_{\mathbf{z}_{kl}^{t,B}} \\ \mathbf{C}_{kl} &= \mathbf{R}_{kl} - \sqrt{\tau_p} \mathbf{W}_{kl}^H \mathbf{R}_{kl} = \mathbb{Q}_{kl}^B \underbrace{\left(\mathbb{\Sigma}_{kl}^B - \tau_p \left(\mathbb{\Sigma}_{kl}^B\right)^2\right)}_{\mathbb{\Psi}_{kl}^B} \mathbb{Q}_{kl}^{B^H} \end{aligned} \tag{27}$$

and finally $\hat{\mathbf{h}}_k^t = [\hat{\mathbf{h}}_{k1}^{t^H} \ \ldots \ \hat{\mathbf{h}}_{kL_k}^{t^H}]^H$ and $\mathbf{C}_k = \text{blkdiag}\{\mathbf{C}_{k1}, \ldots, \mathbf{C}_{kL_k}\}$.

The expression for the receive combiner $\mathbf{v}_k^t$ based on the estimated quantities becomes [43], [44]

$$\begin{aligned} \mathbf{v}_k^t &= \left(\mathbf{R}_{\tau_k} - \tau_p \mathbf{R}_k + \mathbf{C}_k + \hat{\mathbf{h}}_k^t \hat{\mathbf{h}}_k^{t^H}\right)^{-1} \hat{\mathbf{h}}_k^t \\ &= \begin{bmatrix} \mathbb{X}_{k1}^B \left(\mathbf{I}_{R^B} - \tau_p \mathbb{\Sigma}_{k1}^B + \mathbb{\Psi}_{k1}^B\right)^{-1} \mathbf{z}_{k1}^{t,B} \\ \vdots \\ \mathbb{X}_{kL_k}^B \left(\mathbf{I}_{R^B} - \tau_p \mathbb{\Sigma}_{kL_k}^B + \mathbb{\Psi}_{kL_k}^B\right)^{-1} \mathbf{z}_{kL_k}^{t,B} \end{bmatrix} (1 + \alpha_k^t)^{-1} \end{aligned} \tag{28}$$

with

$$\alpha_k^t = \sum_{l \in \mathcal{M}_k} \mathbf{z}_{kl}^{t,B^H} \left(\mathbf{I}_{R^B} - \tau_p \mathbb{\Sigma}_{kl}^B + \mathbb{\Psi}_{kl}^B\right)^{-1} \mathbf{z}_{kl}^{t,B}. \tag{29}$$

Hence, both CE as well as RC can be performed locally, except for the scalar multiplication with $(1 + \alpha_k^t)^{-1}$ in $\mathbf{v}_{kl}^t = \mathbb{X}_{kl}^B (\mathbf{I}_{R^B} - \tau_p \mathbb{\Sigma}_{kl}^B + \mathbb{\Psi}_{kl}^B)^{-1} \mathbf{z}_{kl}^{t,B} (1 + \alpha_k^t)^{-1}$. Therefore, $\alpha_k^t$ needs to be computed using an in-network sum, which is then the only required communication between the APs in the user-centric network $\mathcal{M}_k$[5].

[5] In most applications, e.g., when the spectral efficiency (SE) needs to be maximized, one is already satisfied with a receive combiner up to a multiple of $\mathbf{v}_k^t$. This communication can thus be dropped or embedded in a final single channel equalizer.

### B. LOW RANK $\overline{\mathbf{R}}_k$ WITH USER-CENTRIC RANK $R^L$

In this subsection, a channel model will be assumed where the LoS component dominates the NLoS components and arrives at the serving APs in a coherent way, such that it enforces strong correlation between the channels in the APs in the user-centric network $\mathcal{M}_k$. Hence, a low rank $R^L$ for $\overline{\mathbf{R}}_k$ will be assumed, e.g., $R^L = 1$ or 2 will be able to cover the LoS component (possibly including some early reflections).

The following structure is thus imposed on $\overline{\mathbf{R}}_k$:

$$\overline{\mathbf{R}}_k = \overline{\mathbb{Q}}_k^L \overline{\mathbb{\Sigma}}_k^L \overline{\mathbb{Q}}_k^{L^H} \tag{30}$$

with

$$\overline{\mathbb{Q}}_k^L = [\overline{\mathbb{Q}}_{k1}^{L^H} \ \dots \ \overline{\mathbb{Q}}_{kL_k}^{L^H}]^H \in \mathbb{C}^{NL_k \times R^L}, \ \overline{\mathbb{\Sigma}}_k^L \in \mathbb{C}^{R^L \times R^L}. \tag{31}$$

Since $\overline{\mathbf{R}}_{\tau_k}$ and $\overline{\mathbf{R}}_{all_k}$ are no longer block diagonal, (19) has to be solved by means of a GEVD of the matrix pencil $\{\mathbf{R}_{\tau_k}, \mathbf{R}_{all_k}\}$, i.e. involving all the antenna signals in the user-centric network $\mathcal{M}_k$:

$$\begin{aligned} \mathbf{R}_{\tau_k} &= \mathbf{Q}_k^L \mathbf{Q}_k^{L^H} \\ \mathbf{R}_{all_k} &= \mathbf{Q}_k^L \mathbf{\Sigma}_{all_k}^L \mathbf{Q}_k^{L^H}. \end{aligned} \tag{32}$$

Here $\mathbf{Q}_k^L$ is again an invertible matrix, its Hermitian inverse contains the generalized eigenvectors as columns, and $\mathbf{\Sigma}_{all_k}^L$ is a diagonal matrix containing the inverse of the generalized eigenvalues where the diagonal elements are sorted from small to large. Let $\mathbb{\Sigma}_{all_k}^L$ denote the $R^L \times R^L$ diagonal matrix with the first $R^L$ columns and rows of $\mathbf{\Sigma}_{all_k}^L$. The optimal solution in (19) is then given by

$$\mathbf{R}_k = \mathbb{Q}_k^L \mathbb{\Sigma}_k^L \mathbb{Q}_k^{L^H} \tag{33}$$

where

$$\begin{aligned} \mathbb{\Sigma}_k^L &= \frac{1}{\tau_p - 1} \lfloor \mathbf{I}_{R^L} - \mathbb{\Sigma}_{all_k}^L \rfloor_0 \\ \mathbb{Q}_k^L &= \mathbf{Q}_k^L [\mathbf{I}_{R^L} \ \mathbf{0}_{R^L \times (NL_k - R^L)}]^H. \end{aligned} \tag{34}$$

Also define

$$\mathbb{X}_k^L = \left(\mathbf{Q}_k^L\right)^{-H} [\mathbf{I}_{R^L} \ \mathbf{0}_{R^L \times (NL_k - R^L)}]^H = (\mathbf{R}_{\tau_k})^{-1} \mathbb{Q}_k^L \tag{35}$$

such that $\mathbb{X}_{kl}^{L^H} \mathbb{Q}_{kl}^L = \mathbf{I}_{R^L}$.

The MMSE-based CE filter $\mathbf{W}_k$ with the estimated quantities is then given as

$$\mathbf{W}_k = \sqrt{\tau_p} (\mathbf{R}_{\tau_k})^{-1} \mathbf{R}_k = \sqrt{\tau_p} \mathbb{X}_k^L \mathbb{\Sigma}_k^L \mathbb{Q}_k^{L^H} \tag{36}$$

and the corresponding channel estimates and estimation error covariance are given by

$$\hat{\mathbf{h}}_k^t = \mathbf{W}_k^H \mathbf{y}_{\tau_k}^{\mathcal{M}_k t} = \mathbb{Q}_k^L \underbrace{\sqrt{\tau_p} \mathbb{\Sigma}_k^L \mathbb{X}_k^{L^H} \mathbf{y}_{\tau_k}^{\mathcal{M}_k t}}_{\mathbf{z}_k^{t,L}}$$

$$\mathbf{C}_k = \mathbf{R}_k - \sqrt{\tau_p} \mathbf{W}_k^H \mathbf{R}_k = \mathbb{Q}_k^L \underbrace{\left(\mathbb{\Sigma}_k^L - \tau_p \left(\mathbb{\Sigma}_k^L\right)^2\right)}_{\mathbb{\Psi}_k^L} \mathbb{Q}_k^{L^H}. \tag{37}$$

The receive combiner $\mathbf{v}_k^t$ can be written as

$$\begin{aligned} \mathbf{v}_k^t &= \left(\mathbf{R}_{\tau_k}^{\mathcal{M}_k} - \tau_p \mathbf{R}_k + \mathbf{C}_k + \hat{\mathbf{h}}_k^t \hat{\mathbf{h}}_k^{t,H}\right)^{-1} \hat{\mathbf{h}}_k^t \\ &= \mathbb{X}_k \left(\mathbf{I}_{R^L} - \tau_p \mathbb{\Sigma}_k^L + \mathbb{\Psi}_k^L + \mathbf{z}_k^{t,L} \mathbf{z}_k^{t,L^H}\right)^{-1} \mathbf{z}_k^{t,L}. \end{aligned} \tag{38}$$

The CE and RC can not be performed locally, since the antenna signals $\mathbf{y}^{\mathcal{M}_k t}$ have to be centralized to be able to compute the GEVD of $\overline{\mathbf{R}}_{\tau_k}$ and $\overline{\mathbf{R}}_{all_k}$. However, the expressions show that when $\mathbb{X}_k^{L^H} \mathbf{y}_{\tau_k}^{\mathcal{M}_k t}$ (which contains only $R^L$ channels) and $\mathbb{Q}_{kl}^L$, $\mathbb{X}_{kl}^L$, $\mathbb{\Sigma}_k^L$ are available, the channel estimates and receive combiner ($\hat{\mathbf{h}}_{kl}^t$ and $\mathbf{v}_{kl}^t$) can be computed locally.

### C. SUPERPOSITION OF BLOCK DIAGONAL AND LOW RANK $\overline{\mathbf{R}}_k$

In this subsection, a channel model will be assumed that is a superposition of the channel models assumed in Sections III-A and III-B. It thus allows for both NLoS components enforcing a local rank $R^B$ as well as LoS components enforcing a user-centric rank $R^L$. It encompasses the previous models as special cases, obtained by setting either $R^B$ or $R^L$ equal to 0.

The following structure is imposed on $\overline{\mathbf{R}}_k$:

$$\overline{\mathbf{R}}_k = \underbrace{\overline{\mathbb{Q}}_k^B \overline{\mathbb{\Sigma}}_k^B \overline{\mathbb{Q}}_k^{B^H}}_{\overline{\mathbf{R}}_k^B} + \underbrace{\overline{\mathbb{Q}}_k^L \overline{\mathbb{\Sigma}}_k^L \overline{\mathbb{Q}}_k^{L^H}}_{\overline{\mathbf{R}}_k^L} \tag{39}$$

where $\overline{\mathbb{Q}}_k^B, \overline{\mathbb{\Sigma}}_k^B \ \overline{\mathbb{Q}}_k^L, \overline{\mathbb{\Sigma}}_k^L$ are defined as in (21) and (31).

An algorithm to estimate these terms is provided in Algorithm 1. It is an alternating optimization algorithm that minimizes the following objective for $\boldsymbol{R}_k^B$ and $\boldsymbol{R}_k^L$:

$$\|\mathbf{R}_{\tau_k}^{-1/2} \left(\mathbf{R}_{\tau_k} - \mathbf{R}_{all_k} - (\tau_p - 1)(\boldsymbol{R}_k^B + \boldsymbol{R}_k^L)\right) \mathbf{R}_{\tau_k}^{-H/2}\|_F^2 \tag{40}$$

where the structure of $\boldsymbol{R}_k^B$ and $\boldsymbol{R}_k^L$ is given by (39). Convergence of Algorithm 1 can be proven by arguing that every step of the algorithm decreases the objective function and the objective function is bounded from below by 0. Hence, after convergence, a limit point of (40) must be reached.

**Algorithm 1:** Rank $\{R^B, R^L\}$ GEVD-Based Channel Covariance Estimation.

1: Set $n \leftarrow 0$ and initialize $\mathbf{R}_k^{B,0}$ as $\mathbf{0}_{NL_k \times NL_k}$.
2: Solve (40) for $\mathbf{R}_k^L$ with $\mathbf{R}_k^B = \mathbf{R}_k^{B,n}$ fixed. The solution is given by performing the GEVD [42]:

$$\begin{aligned} \mathbf{R}_{\tau_k} &= \mathbf{Q}_k^{L,n} \mathbf{Q}_k^{L,n^H} \\ \mathbf{R}_{all_k} + (\tau_p - 1)\mathbf{R}_k^{B,n} &= \mathbf{Q}_k^{L,n} \mathbf{\Sigma}_{all_k}^{L,n} \mathbf{Q}_k^{L,n^H} \end{aligned} \tag{41}$$

where $\mathbb{\Sigma}_{all_k}^{L,n}$ is defined as before. The optimal solution is then given as

$$\mathbb{\Sigma}_k^{L,n+1} = \frac{1}{\tau_p - 1} \lfloor \mathbf{I}_{R^L} - \mathbb{\Sigma}_{all_k}^{L,n} \rfloor_0 \tag{42}$$

$$\mathbb{Q}_k^{L,n+1} = \mathbf{Q}_k^{L,n}[\mathbf{I}_{R^L}\ \mathbf{0}_{R^L\times NL_k-R^L}]^H \tag{43}$$

$$\mathbb{X}_k^{L,n+1} = \mathbf{R}_{\tau_k}^{-1}\mathbb{Q}_k^{L,n+1} \tag{44}$$

$$\mathbf{R}_k^{L,n+1} = \mathbb{Q}_k^{L,n+1}\mathbb{\Sigma}_k^{L,n+1}\mathbb{Q}_k^{L,n+1^H}. \tag{45}$$

3: For $\tilde{l} \in \{1,\ldots,L_k\}$:

- Solve (40) for $\mathbf{R}_{kl}^B$ with $\mathbf{R}_{k\tilde{l}}^B\ \forall \tilde{l} \neq l$ and $\mathbf{R}_k^L$ fixed. This can be accomplished by setting $\mathbf{R}_k^B = \mathbf{H}_{kl}\mathbf{R}_{kl}^B\mathbf{H}_{kl}^H + \mathbf{R}_{k,-l}^B$ where $\mathbf{R}_{k,-l}^B$ is a block diagonal matrix containing a zero-block on the position of $\mathbf{R}_{kl}^B$, $\mathbf{R}_{k\tilde{l}}^B = \mathbf{R}_{k\tilde{l}}^{B,n+1}\ \forall \tilde{l} < l$, $\mathbf{R}_{k\tilde{l}}^B = \mathbf{R}_{k\tilde{l}}^{B,n}\ \forall \tilde{l} > l$ and $\mathbf{R}_k^L = \mathbf{R}_k^{L,n+1}$. The problem is then optimally solved using a prior knowledge GEVD (PK-GEVD) [39]:

$$\mathbf{H}_{kl} = \begin{bmatrix}\mathbf{0}_{N\times N(l-1)} & \mathbf{I}_N & \mathbf{0}_{N\times N(L_k-l-1)}\end{bmatrix}^H \tag{46}$$

$$\mathbf{B}_{kl} = \begin{bmatrix}\mathbf{I}_{N(l-1)} & \mathbf{0}_{N(l-1)\times N} & \mathbf{0} \\ \mathbf{0} & \mathbf{0}_{N(L_k-1)\times N} & \mathbf{I}_{N(L_k-l-1)}\end{bmatrix}^H \tag{47}$$

$$\mathbf{F}_{kl} = \mathbf{H}_{kl} - \mathbf{B}_{kl}\left(\mathbf{B}_{kl}^H\mathbf{R}_{\tau_k}\mathbf{B}_{kl}\right)^{-1}\mathbf{B}_{kl}^H\mathbf{R}_{\tau_k}\mathbf{H}_{kl} \tag{48}$$

$$\begin{aligned}&\mathbf{F}_{kl}^H\mathbf{R}_{\tau_k}\mathbf{F}_{kl} = \mathbf{Q}_{kl}^{B,n}\mathbf{Q}_{kl}^{B,n^H} \\ &\mathbf{F}_{kl}^H\left(\mathbf{R}_{all_k} + (\tau_p-1)\left(\mathbf{R}_k^{L,n+1} + \mathbf{R}_{k,-l}^B\right)\right)\mathbf{F}_{kl} \\ &\quad = \mathbf{Q}_{kl}^{B,n}\mathbf{\Sigma}_{all_k,l}^{B,n}\mathbf{Q}_{kl}^{B,n^H}\end{aligned} \tag{49}$$

where $\mathbb{\Sigma}_{all_kl}^{B,n}$ is defined as before. The optimal solution is then given as

$$\mathbb{\Sigma}_{kl}^{B,n+1} = \frac{1}{\tau_p-1}\lfloor\mathbf{I}_{R^B} - \mathbb{\Sigma}_{all_kl}^{B,n}\rfloor_0 \tag{50}$$

$$\mathbb{Q}_{kl}^{B,n+1} = \mathbf{Q}_{kl}^{B,n}[\mathbf{I}_{R^B}\ \mathbf{0}_{R^B\times N-R^B}]^H \tag{51}$$

$$\mathbb{X}_{kl}^{B,n+1} = \left(\mathbf{R}_{\tau_k l} - \tau_p\mathbb{Q}_{kl}^{L,n+1}\mathbb{\Sigma}_k^{L,n+1}\mathbb{Q}_{kl}^{L,n+1^H}\right)^{-1}\mathbb{Q}_{kl}^{B,n+1}$$

$$\mathbf{R}_{kl}^{B,n+1} = \mathbb{Q}_{kl}^{B,n+1}\mathbb{\Sigma}_{kl}^{B,n+1}\mathbb{Q}_{kl}^{B,n+1^H}. \tag{52}$$

4: $n \leftarrow n+1$ and return to step 2.

Algorithm 1 also defines the following quantities:

$$\begin{aligned}\mathbb{X}_{kl}^B &= \left(\mathbf{R}_{\tau_k l} - \tau_p\mathbb{Q}_{kl}^L\mathbb{\Sigma}_k^L\mathbb{Q}_{kl}^{L^H}\right)^{-1}\mathbb{Q}_{kl}^B,\ l = 1,\ldots,L_k \\ \mathbb{X}_k^L &= [\mathbb{X}_{k1}^{L^H}\ \ldots\ \mathbb{X}_{kL_k}^{L^H}]^H = \mathbf{R}_{\tau_k}^{-1}\mathbb{Q}_k^L.\end{aligned} \tag{53}$$

It is assumed that, upon convergence of Algorithm 1, $\mathbf{R}_{\tau_k} - \tau_p\mathbb{Q}_k^L\mathbb{\Sigma}_k^L\mathbb{Q}_k^{L^H}$ can be approximated by a block diagonal matrix,[6] sot that the following identity is assumed to be valid:

$$\left(\mathbf{R}_{\tau_k} - \tau_p\mathbb{Q}_k^L\mathbb{\Sigma}_k^L\mathbb{Q}_k^{L^H}\right)^{-1}\mathbf{Q}_k^B \approx \mathbb{X}_k^B. \tag{54}$$

with $\mathbb{X}_k^B = \text{blkdiag}\{\mathbb{X}_{k1}^B,\ldots,\mathbb{X}_{kL_k}^B\}$.

Based on the approximation in (54), the CE filter can be written as

$$\begin{aligned}\mathbf{W}_k &= \sqrt{\tau_p}\mathbf{R}_{\tau_k}^{-1}\mathbf{R}_k = \sqrt{\tau_p}\mathbf{R}_{\tau_k}^{-1}(\mathbf{Q}_k^B\mathbf{\Sigma}_k^B\mathbf{Q}_k^{B^H} + \mathbb{Q}_k^L\mathbb{\Sigma}_k^L\mathbb{Q}_k^{L^H}) \\ &\approx \sqrt{\tau_p}\mathbb{X}_k^B\mathbf{\Sigma}_k^B\mathbf{Q}_k^{B^H} + \sqrt{\tau_p}\mathbb{X}_k^L\mathbb{\Sigma}_k^L\dot{\mathbb{Q}}_k^H\end{aligned} \tag{55}$$

with

$$\begin{aligned}\dot{\mathbb{Q}}_k &\triangleq \mathbb{Q}_k^L - \tau_p\mathbf{Q}_k^B\mathbf{\Sigma}_k^B\mathbf{Q}_k^{B^H}\mathbb{X}_k^L\left(\mathbf{I}_{R^L} - \tau_p\mathbb{\Sigma}_k^L\right)^{-1} \\ &= \mathbb{Q}_k^L - \tau_p\mathbf{Q}_k^B\mathbf{\Sigma}_k^B\mathbb{X}_k^{B^H}\mathbb{Q}_k^L.\end{aligned} \tag{56}$$

A proof for (55) can be found in Appendix A. The equality in (56) can be derived by multiplying (85) with $\mathbf{Q}_k^{B^H}$.

The corresponding channel estimates and estimation error covariance are given by

$$\begin{aligned}\hat{\mathbf{h}}_k^t &\approx \mathbf{Q}_k^B\underbrace{\sqrt{\tau_p}\mathbf{\Sigma}_k^B\mathbb{X}_k^{B^H}\mathbf{y}_{\tau_k}^{\mathcal{M}_k t}}_{\mathbf{z}_k^{t,B}} + \dot{\mathbb{Q}}_k\underbrace{\sqrt{\tau_p}\mathbb{\Sigma}_k^L\mathbb{X}_k^{L^H}\mathbf{y}_{\tau_k}^{\mathcal{M}_k t}}_{\mathbf{z}_k^{t,L}} \\ \mathbf{C}_k &\approx \mathbf{Q}_k^B\underbrace{\left(\mathbf{\Sigma}_k^B - \tau_p\left(\mathbf{\Sigma}_k^B\right)^2\right)}_{\mathbf{\Psi}_k^B}\mathbf{Q}_k^{B^H} + \dot{\mathbb{Q}}_k\underbrace{\left(\mathbb{\Sigma}_k^L - \tau_p\left(\mathbb{\Sigma}_k^L\right)^2\right)}_{\mathbb{\Psi}_k^L}\dot{\mathbb{Q}}_k^H.\end{aligned} \tag{57}$$

This last approximation can be obtained by combining $\mathbf{C}_k = \mathbf{R}_k - \sqrt{\tau_p}\mathbf{W}_k^H\mathbf{R}_k$ with (21), (55) and (56).

Note that $\dot{\mathbb{Q}}_k = [\dot{\mathbb{Q}}_{k1}^H\ \ldots\ \dot{\mathbb{Q}}_{kL_k}^H]^H$ with

$$\dot{\mathbb{Q}}_{kl} = \mathbb{Q}_{kl}^L - \tau_p\mathbb{Q}_{kl}^B\mathbb{\Sigma}_{kl}^B\mathbb{X}_{kl}^{B^H}\mathbb{Q}_{kl}^L \tag{58}$$

and thus

$$\hat{\mathbf{h}}_{kl}^t \approx \mathbb{Q}_{kl}^B\underbrace{\sqrt{\tau_p}\mathbb{\Sigma}_{kl}^B\mathbb{X}_{kl}^{B^H}\mathbf{y}_{\tau_k l}^t}_{\mathbf{z}_{kl}^{t,B}} + \dot{\mathbb{Q}}_{kl}\mathbf{z}_k^{t,L} \tag{59}$$

$$\mathbf{C}_{kl} \approx \mathbb{Q}_{kl}^B\underbrace{\left(\mathbb{\Sigma}_{kl}^B - \tau_p\left(\mathbb{\Sigma}_{kl}^B\right)^2\right)}_{\mathbf{\Psi}_k^B}\mathbb{Q}_k^{B^H} + \dot{\mathbb{Q}}_{kl}\mathbb{\Psi}_k^L\dot{\mathbb{Q}}_{kl}^H. \tag{60}$$

This shows that only a subset of the estimation quantities ($\mathbb{Q}_{kl}^B$, $\mathbb{\Sigma}_{kl}^B$, $\mathbb{X}_{kl}^{B^H}$, $\dot{\mathbb{Q}}_{kl}$, $\mathbb{\Sigma}_{kl}^B$) and $\mathbb{X}_k^{L^H}\mathbf{y}_{\tau_k}^{\mathcal{M}_k t}$ are needed to compute local channel estimates. Note that the quantities $\mathbb{Q}_{kl}^B$ and $\dot{\mathbb{Q}}_{kl}$ define the allowed subspace for the channel estimates (as in (59)) coming from respectively the block-diagonal and low-rank component in (39).

The expression for the receive combiner $\mathbf{v}_k^t$ is given in (66) on the next page, where the matrix inversion lemma is used to rewrite the equation. The following identities, avoiding the inversion of $\mathbf{B}_k$, are also approximately valid (assuming that $\mathbf{B}_k$ is block diagonal)

$$\mathbf{B}_k^{-1}\mathbf{Q}_k^B\mathbf{z}_k^{t,B} \approx \mathbb{X}_k^B\left(\mathbf{I}_{L_kR^B} + \mathbb{\Sigma}_k^B - \tau_p\mathbf{\Sigma}_k^B - \tau_p\left(\mathbb{\Sigma}_k^B\right)^2\right)^{-1}\mathbf{z}_k^{t,B}$$

[6] Referring to (10), this is only the case if $\overline{\mathbf{R}}_{\mathbf{nn}}^{\mathcal{M}_k}$ and $\overline{\mathbf{R}}_{\tilde{k}}^{\mathcal{M}_k}$ for all $\tilde{k} \neq k$ are block diagonal. If this is not the case, then this matrix will no longer be block diagonal and the provided formulas only hold as approximations. However, as the simulations will show, the resulting CE and RC are still performing well.

$$\mathbf{B}_k^{-1}\dot{\mathbb{Q}}_k \approx \mathbb{X}_k^L \left(\mathbf{I}_{R^L} - \tau_p \mathbb{Z}_k^L\right)^{-1} - \mathbf{X}_k^B \left(\mathbf{I}_{L_k R^B} + \left(\mathbf{\Sigma}_k^B\right)^{-1}\right)^{-1} \mathbf{X}_k^{B^H} \mathbb{Q}_k^L \quad (61)$$

and the $l$th block row can consequently be written as

$$[\mathbf{B}_k^{-1}\mathbf{Q}_k^B \mathbf{z}_k^{t,B}]_l \approx \mathbb{X}_{kl}^B \left(\mathbf{I}_{R^B} + \mathbb{Z}_{kl}^B - \tau_p \mathbb{Z}_{kl}^B - \tau_p \left(\mathbb{Z}_{kl}^B\right)^2\right)^{-1} \mathbf{z}_{kl}^{t,B}$$

$$[\mathbf{B}_k^{-1}\dot{\mathbb{Q}}_k]_l \approx \mathbb{X}_{kl}^L \left(\mathbf{I}_{R^L} - \tau_p \mathbb{Z}_k^L\right)^{-1} - \mathbb{X}_{kl}^B \left(\mathbf{I}_{R^B} + \left(\mathbb{Z}_{kl}^B\right)^{-1}\right)^{-1} \mathbb{X}_{kl}^{B^H} \mathbb{Q}_{kl}^L. \quad (62)$$

The following quantities are also used in (66) shown at the bottom of this page and they can be simplified as

$$\alpha_k^t = \mathbf{z}_k^{t,B^H} \mathbb{Q}_k^{B^H} \mathbf{B}_k^{-1} \mathbb{Q}_k^B \mathbf{z}_k^{t,B} \quad (63)$$

$$= \sum_{l \in \mathcal{M}_k} \mathbf{z}_{kl}^{t,B^H} \left(\mathbf{I}_{R^B} + \mathbb{Z}_{kl}^B - \tau_p \mathbb{Z}_{kl}^B - \tau_p \left(\mathbb{Z}_{kl}^B\right)^2\right)^{-1} \mathbf{z}_{kl}^{t,B}$$

$$\boldsymbol{\beta}_k^t = \dot{\mathbb{Q}}_k^H \mathbf{B}_k^{-1} \mathbb{Q}_k^B \mathbf{z}_k^{t,B} \quad (64)$$

$$= \sum_{l \in \mathcal{M}_k} \mathbb{Q}_{kl}^{L^H} \mathbb{X}_{kl}^B \left(\mathbf{I}_{R^B} + \mathbb{Z}_{kl}^B\right)^{-1} \mathbf{z}_{kl}^{t,B}$$

$$\mathbf{\Gamma}_k = \dot{\mathbb{Q}}_k^H \mathbf{B}_k^{-1} \dot{\mathbb{Q}}_k^H = \left(\mathbf{I}_{R^L} - \tau_p \mathbb{Z}_k^L\right)^{-1} - (1+\tau_p) \sum_{l \in \mathcal{M}_k} \mathbb{Q}_{kl}^{L^H} \mathbb{X}_{kl}^B \left(\mathbf{I}_{R^B} + \left(\mathbb{Z}_{kl}^B\right)^{-1}\right)^{-1} \mathbb{X}_{kl}^{B^H} \mathbb{Q}_{kl}^L. \quad (65)$$

The local version of the receive combiner $\mathbf{v}_{kl}^t$ is then provided in (67) shown at the bottom of this page.

Similar to Section III-B, the CE and RC can not be performed locally since $\mathbf{R}_{\tau_k}$ and $\mathbf{R}_{all_k}$ are required for Algorithm 1. However, the expressions show that when $\mathbb{X}_k^{L^H} \mathbf{y}_{\tau_k}^{\mathcal{M}_k t}$ (which only contains $R^L$ signals) and other local quantities are available together with $\alpha_k^t$, $\boldsymbol{\beta}_k^t$, $\mathbf{\Gamma}_k$ as in (63)–(65) (which can be computed using in-network sums), the channel estimates $\hat{\mathbf{h}}_{kl}^t$ and receive combiner $\mathbf{v}_{kl}^t$ can still be computed locally. This will be exploited in the distributed algorithm presented in the next section.

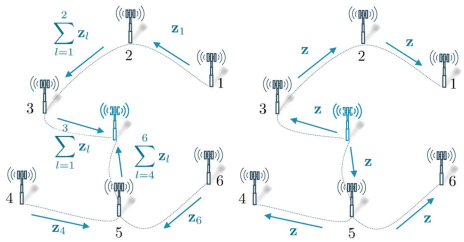

**FIGURE 3.** Tree based in-network sums for user-centric CFmMIMO using 2 phases: (i) in-network summation towards root-AP and (ii) broadcast of sum by root-AP.

## IV. DISTRIBUTED GEVD-BASED CE AND RC

To avoid having to transmit all $NL_k$ antenna signals in $\mathbf{y}^{\mathcal{M}_k t}$ to a central processing unit in the user-centric network $\mathcal{M}_k$, a distributed algorithm is presented in this section that converges (under certain conditions) to the same solution as the centralized GEVD-based CE and RC, discussed in Section III. Since the models in Sections III-A and III-B are special cases of the model in Section III-C, the distributed algorithm will only be presented for the latter model.

To organize the inter-AP communication in an efficient way, the user-centric network $\mathcal{M}_k$ should be able to perform in-network sums for UE $k$, i.e., it should be able to compute $\sum_{l \in \mathcal{M}_k} \mathbf{z}_l$ where $\mathbf{z}_l$ is a certain quantity or parameter. Methods to obtain in-network sums with minimal communication requirements are available in the literature, e.g., relying on consensus or gossip methods [45], [46]. However, these methods typically need many iterations to converge, as well as multiple broadcasts of intermediate summed quantities. Therefore, based on [37], a method is presented to calculate the in-network sums which relies on a tree topology that is formed using the set of available links in the user-centric network with minimal communication requirements (only two transmissions for each link). Note that any connected network (e.g., fully-connected, ring-topology,...) can be pruned to a tree topology, thus this approach works for any connected topology. Fig. 3 explains the organization of the communication.

For the CE, the proposed algorithm requires computing the in-network sum of $R^L \tau_p$ signals received during the pilot phase of each coherence block and $R^L \times R^L$ parameters per iteration. For the RC, the proposed algorithm requires

$$\mathbf{v}_k^t = \Big(\underbrace{\mathbf{R}_{\tau_k} - \tau_p \mathbb{Q}_k^L \mathbb{Z}_k^L \mathbb{Q}_k^{L^H} + \mathbf{Q}_k^B \left(-\tau_p \mathbf{\Sigma}_k^B + \mathbf{\Psi}_k^B\right) \mathbf{Q}_k^{B^H}}_{\mathbf{B}_k} + \dot{\mathbb{Q}}_k \mathbb{\Psi}_k^L \dot{\mathbb{Q}}_k^H + \left[\mathbf{Q}_k^B \mathbf{z}_k^{t,B} \; \dot{\mathbb{Q}}_k\right] \left[1 \mathbf{z}_k^{t,L}\right] \begin{bmatrix} 1 \\ \mathbf{z}_k^{t,L} \end{bmatrix}^H \left[\mathbf{Q}_k^B \mathbf{z}_k^{t,B} \; \dot{\mathbb{Q}}_k\right]^H \Big)^{-1} \left[\mathbf{Q}_k^B \mathbf{z}_k^{t,B} \; \dot{\mathbb{Q}}_k\right] \begin{bmatrix} 1 \\ \mathbf{z}_k^{t,L} \end{bmatrix}$$

$$= \mathbf{B}_k^{-1} [\mathbf{Q}_k^B \mathbf{z}_k^{t,B} \; \dot{\mathbb{Q}}_k] \left(\mathbf{I}_{1+R^L} + \begin{bmatrix} 1 & \mathbf{z}_k^{t,L^H} \\ \mathbf{z}_k^{t,L} & \mathbf{z}_k^{t,L} \mathbf{z}_k^{t,L^H} + \mathbb{\Psi}_k^L \end{bmatrix} \begin{bmatrix} \alpha_k^t & \boldsymbol{\beta}_k^{t^H} \\ \boldsymbol{\beta}_k^t & \mathbf{\Gamma}_k \end{bmatrix}\right)^{-1} \begin{bmatrix} 1 \\ \mathbf{z}_k^{t,L} \end{bmatrix} \quad (66)$$

$$\mathbf{v}_{kl}^t = \mathbf{B}_{kl}^{-1} [\mathbf{Q}_{kl}^B \mathbf{z}_{kl}^{t,B} \; \dot{\mathbb{Q}}_{kl}] \left(\mathbf{I}_{1+R^L} + \begin{bmatrix} 1 & \mathbf{z}_k^{t,L^H} \\ \mathbf{z}_k^{t,L} & \mathbf{z}_k^{t,L} \mathbf{z}_k^{t,L^H} + \mathbb{\Psi}_k^L \end{bmatrix} \begin{bmatrix} \alpha_k^t & \boldsymbol{\beta}_k^{t^H} \\ \boldsymbol{\beta}_k^t & \mathbf{\Gamma}_k \end{bmatrix}\right)^{-1} \begin{bmatrix} 1 \\ \mathbf{z}_k^{t,L} \end{bmatrix} \quad (67)$$

computing the in-network sum of $(1+R^L)\times(1+R^L)$ parameters for each coherence block. Each AP also has to perform computations on a smaller number of input signals, i.e., only the local antenna signals and a compressed $R^L$ dimensional-version of the antenna signals of the other APs. The algorithm is referred to as the rank $\{R^B, R^L\}$ GEVD-based distributed user-centric CE and RC (DUCERC) algorithm and can be related to the distributed algorithms referred to as DANSE, TI-DANSE and GEVD-DANSE of [36], [37], [38] designed for wireless sensor networks. The DUCERC algorithm has a slower adaptation and tracking speed compared to the centralized GEVD-based CE and RC, as it requires multiple iterations on the same data to converge to a stationary solution. However, since the channel covariances are changing, this will allow for an efficient tracking of these changes if different iterations are performed on consecutive data segments.

### A. ALGORITHM DESCRIPTION

The rank $\{R^B, R^L\}$ GEVD-based DUCERC algorithm is presented in Algorithm 2. This is a block-iterative round-robin algorithm,[7] where the updating AP (denoted by index $q$) performs similar operations as in Algorithm 1 using data of $T$ coherence blocks. A token is then passed to the next AP, becoming the new updating AP, and this is continued in a cyclic manner.

In one iteration $n$, each AP compresses the received signals $\mathbf{y}_l^t$ during the pilot phase with $\mathbf{F}_{kl}^n \in \mathbb{C}^{N\times R^L}$ to obtain $\chi_{kl}^t$ as in (68). Using in-network sums and after subtracting its own compressed channel as in (69), it receives a new $R^L$-dimensional channel $\chi_{k,-l}^t$ which it appends to its local antenna signal to obtain the local extended antenna signal $\tilde{\mathbf{y}}_l^t = [\mathbf{y}_l^{tH}\ \chi_{k,-l}^{tH}]^H$. This extended antenna signal is then used to perform one iteration of Algorithm 1 (one GEVD and one PK-GEVD). To this end, the updating AP needs an estimate of the block diagonal component present in $\chi_{k,-l}^t$, which is given by $\xi_{k,-l}^n = \sum_{l\in\mathcal{M}_k\setminus\{q\}} \mathbf{F}_{kl}^{nH}\mathbf{R}_{kl}^{B,n}\mathbf{F}_{kl}^n$ and is easily computed using in-network sums. The compression matrix of the updating AP $q$ is then updated as in (72).

The local GEVD results in the extended solutions $\tilde{\mathbb{Q}}_{kq}^{L,n+1}, \tilde{\mathbb{X}}_{kq}^{L,n+1}$. The first $N$ rows then correspond to local estimates of $\mathbb{Q}_{kq}^{L,n+1}, \mathbb{X}_{kq}^{L,n+1}$, which are required for the CE and RC as noted in Section III. The local PK-GEVD directly results in $\mathbb{Q}_{kq}^{B,n+1}, \mathbb{\Sigma}_{kq}^{B,n+1}, \mathbb{X}_{kq}^{B,n+1}$ and $\mathbf{R}_{kq}^{B,n+1}$, which are also required for the CE and RC. CE and RC can then be performed as presented in step 5. RC requires knowledge of $\alpha_k^t, \boldsymbol{\beta}_k^t, \boldsymbol{\Gamma}_k$ for each coherence block, which can be computed using in-network sums as in (63)–(65) by replacing the centralized solutions with the solutions in the current iteration.

[7]Instead of round-robin updates, asynchronous updating as discussed in [36] can also be performed, but this is not discussed here for ease of exposition.

**Algorithm 2:** Rank $\{R^B, R^L\}$ GEVD-Based Distributed User-Centric CE and RC (DUCERC).

1: Set $n \leftarrow 0, q \leftarrow 1$ and initialize $\mathbf{F}_{kl}^0, \forall l \in \mathcal{M}_k$ randomly.

2: - Each AP $l \in \mathcal{M}_k$ compresses $T\tau_p$ pilot signals of $T$ coherence blocks to $\chi_{kl}^n \in \mathbb{C}^{R^L}$:

$$\chi_{kl}^t = \mathbf{F}_{kl}^{nH}\mathbf{y}_l^t. \tag{68}$$

- The network is used to construct $T\tau_p$ in-network sum $\sum_{l\in\mathcal{M}_k}\chi_{kl}^t$ and each AP $l \in \mathcal{M}_k$ subtracts its compressed version from this to obtain

$$\chi_{k,-l}^t = \sum_{l\in\mathcal{M}_k}\chi_{kl}^t - \chi_{kl}^t \tag{69}$$

and appends this to its antenna signal $\tilde{\mathbf{y}}_l^t = [\mathbf{y}_l^{tH}\ \chi_{k,-l}^{tH}]^H$.
- The network is also used to construct the in-network sum

$$\xi_k^n = \sum_{l\in\mathcal{M}_k}\mathbf{F}_{kl}^{nH}\mathbf{R}_{kl}^{B,n}\mathbf{F}_{kl}^n \in \mathbb{C}^{R^L\times R^L}. \tag{70}$$

3: At update AP $q$:
- Set $\tilde{\mathbf{R}}_{kq}^{B,n} = \text{blkdiag}\{\mathbf{R}_{kq}^{B,n}, \xi_{k,-q}^n\}$ with $\xi_{k,-q}^n = \xi_k^n - \mathbf{F}_{kq}^{nH}\mathbf{R}_{kq}^{B,n}\mathbf{F}_{kq}^n$ and compute $\tilde{\mathbf{R}}_{\tau_k q}, \tilde{\mathbf{R}}_{all_k q}$ from $\tilde{\mathbf{y}}_q^t$.
- Compute $\tilde{\mathbb{Q}}_{kq}^{L,n+1}, \mathbb{\Sigma}_{kq}^{L,n+1}, \tilde{\mathbb{X}}_{kq}^{L,n+1}$ and $\tilde{\mathbf{R}}_{kq}^{L,n+1}$ form the GEVD of $\{\tilde{\mathbf{R}}_{\tau_k q}, \tilde{\mathbf{R}}_{all_k q} + (\tau_p - 1)\tilde{\mathbf{R}}_{kq}^{B,n}\}$ similar as in (42)–(45).
- Compute $\mathbb{Q}_{kq}^{B,n+1}, \mathbb{\Sigma}_{kq}^{B,n+1}, \mathbb{X}_{kq}^{B,n+1}$ and $\mathbf{R}_{kq}^{B,n+1}$ from the PK-GEVD of $\{\tilde{\mathbf{R}}_{\tau_k q}, \tilde{\mathbf{R}}_{all_k q} + (\tau_p - 1)(\tilde{\mathbf{R}}_{kq}^{L,n+1} + \tilde{\mathbf{R}}_{k,-q}^{B,n})\}$ similar as in (50)–(52) with

$$\tilde{\mathbf{H}}_{kq} = [\mathbf{I}_N\ \mathbf{0}_{N\times R^L}]^H,\ \tilde{\mathbf{B}}_{kq} = [\mathbf{0}_{R^L\times N}\ \mathbf{I}_{R^L}]^H \tag{71}$$

and $\dot{\mathbb{Q}}_{kq}^{n+1} = \mathbb{Q}_{kq}^{L,n+1} - \tau_p\mathbb{Q}_{kq}^{B,n+1}\mathbb{\Sigma}_{kq}^{B,n+1}\mathbb{X}_{kq}^{B,n+1}\mathbb{Q}_{kq}^{L,n+1}$.
- Update the compression matrix as

$$\mathbf{F}_{kq}^{n+1} = \mathbb{X}_{kq}^{L,n+1}\left(\mathbb{X}_{k,-q}^{L,n+1}\right)^{-1} \tag{72}$$

with $\mathbb{X}_{k,-q}^{L,n+1} = [\mathbf{0}_{R^L\times N}\ \mathbf{I}_{R^L}]\tilde{\mathbb{X}}_{kq}^{L,n+1}$.

4: Other APs $l \in \mathcal{M}_k \setminus \{q\}$ copy its previous quantities, i.e., $\tilde{\mathbb{Q}}_{kl}^{L,n+1} = \tilde{\mathbb{Q}}_{kl}^{L,n}$ etc.

5: - Each AP $l \in \mathcal{M}_k$ computes channels estimates for $t = 1\ldots T$

$$\begin{aligned}\mathbf{z}_{kl}^{t,B} &= \sqrt{\tau_p}\mathbb{\Sigma}_{kl}^{B,n+1}\mathbb{X}_{kl}^{B,n+1H}\mathbf{y}_{\tau_k l}^t\\ \mathbf{z}_{kl}^{t,L} &= \sqrt{\tau_p}\tilde{\mathbb{\Sigma}}_{kl}^{L,n+1}\tilde{\mathbb{X}}_{kl}^{L,n+1H}\tilde{\mathbf{y}}_{\tau_k}^t\\ \mathbf{h}_{kl}^t &= \mathbb{Q}_{kl}^{B,n+1}\mathbf{z}_{kl}^{t,B} + \dot{\mathbb{Q}}_{kl}^{n+1}\mathbf{z}_k^{t,L}.\end{aligned} \tag{73}$$

- The network is used to construct $\alpha_k^t, \boldsymbol{\beta}_k^t, \boldsymbol{\Gamma}_k$ as in (63)–(65) for $t = 1\ldots T$.
- Each AP $l \in \mathcal{M}_k$ compute the receive combiner $\mathbf{v}_{kl}^t$ as in (67) for $t = 1\ldots T$.
- The receive combiners are then used to obtain estimates of the data transmitted by UE $k$ during the UL data transmission phase as $\hat{s}_k = \sum_{l\in\mathcal{M}_k}\mathbf{v}_{kl}^{tH}\mathbf{y}_l$.

6: $n \leftarrow n+1, q \leftarrow (q \mod L_k)+1$ and return to step 2.

### B. CONVERGENCE ANALYSIS

The proposed algorithm is a combination of the DACGEE algorithm proposed in [47] and PK-GEVD-DANSE in [39]. DACGEE assumes a fully-connected network, whereas the current algorithm uses in-network sums as a communication protocol, which reduces the communication overhead and makes the algorithm topology-independent since any connected network can be pruned to a tree [48]. The following theorem can then be stated.

*Theorem IV.1:* If

- at a certain iteration $\tilde{n}$ $\mathbf{R}_k^{B,\tilde{n}}$ is kept fixed, i.e., the third bullet in step 3 of Algorithm 2 is not executed or results in the same solution,
- $\mathbf{R}_{\tau_k}$, $\mathbf{R}_{all_k}$ are invertible,
- $\tilde{\mathbf{R}}_{\tau_k q}$, $\tilde{\mathbf{R}}_{all_k q}$ are perfectly estimated using an infinite observation window in each iteration,

then the DUCERC algorithm converges for any initialization of its parameters to the solution provided in Section III-C, i.e., when $n \to \infty$ and $\forall l \in \mathcal{M}_k$, $\mathbb{X}_{kl}^{L,n} = \mathbb{X}_{kl}^{L}$, $\mathbb{Q}_{kl}^{L,n} = \mathbb{Q}_{kl}^{L}$, $\mathbb{\Sigma}_{kq}^{L,n} = \mathbb{\Sigma}_{q}^{L}$ with $\mathbf{R}_k^B = \mathbf{R}_k^{B,\tilde{n}}$. The corresponding CE and RC then also converge since DUCERC uses distributed versions of the expressions in Section III-C.

*Proof:* See Appendix B.

To prove convergence of DUCERC to the same solution as Algorithm 1, it should also be proven that for a fixed $\mathbf{R}_k^{L,\tilde{n}}$, the DUCERC algorithm converges. However, as shown in [39], this will require compression of the local antenna signals to $2R^B$ channels and this for each $l \in \mathcal{M}_k$. Since $R^B$ is typically $N/2$, this will not result in a communication cost reduction. Therefore, this is replaced by the proposed heuristic solution in the third bullet of step 3, which does not require any extra communication and assumes that the compressed signals of the other APs contain only noise references [39] to determine the local block diagonal component $\mathbf{R}_{kl}$. This is reflected in the local subspace and blocking matrices $\tilde{\mathbf{H}}_{kq}$ and $\tilde{\mathbf{B}}_{kq}$ defined in (71) (see [39] for further details). Hence, convergence cannot be shown for this algorithm, but simulations will show that the algorithm still provides similar performance as the centralized solution.

### C. COMMUNICATION COST

The communication cost of the DUCERC algorithm is determined by the following in-network sums:

- $R^L \tau_p$ signals received during the pilot phase of each coherence block,
- $R^L \times R^L$ parameters[8] per iteration to compute $\xi_k^n$ for the user-centric GEVD,
- $(1 + R^L) \times (1 + R^L)$ parameters $(\alpha_k^t, \boldsymbol{\beta}_k^t, \boldsymbol{\Gamma}_k)$ for the RC in each coherence block.

Moreover, there is also the need for in-network sums of $\tau_u$ signals received during the UL data transmission phase of each coherence block. This should be compared to having to transmit all $NL_k\tau_p$ signals received during the pilot phase of each coherence block to a central processing unit in the network. This central central processing unit then computes all quantities as in Section III-C, and transmits $\mathbf{v}_{kl}^t$ back to each AP for the RC phase. It is clear that when $R^L$ is small (e.g., one or two), the DUCERC algorithm achieves a large communication cost reduction. Also the computations are done in the network using smaller input signals, so there is no need for a strong centralized processing unit.

Note that the communication cost is even more reduced for the channel models presented in Section III-A and III-B. In the first case, $R^L = 0$, so the only necessary communication will be $\alpha_k^t$ during each coherence block. In the second case, $\chi_k^n$, $\alpha_k^t$, $\boldsymbol{\beta}_k^t$ will be zero, and $\boldsymbol{\Gamma}_k$ consists of quantities that are locally available, so only the $R^L\tau_p$ signals received during the pilot phase of each coherence block must be communicated.

### D. COMPUTATIONAL COMPLEXITY

The computational complexity of the DUCERC algorithm is dominated by the GEVD, PK-GEVD and matrix inversion in step 3. The computational complexity of these operations scale as $O(M^3)$ with $M$ the dimension of the matrix. Note that, compared to Algorithm 1 where the matrices have dimension $NL_k \times NL_k$, the current matrices have dimension $(N + R^L) \times (N + R^L)$ resulting in a strong computational complexity reduction. This implies less stringent requirements on the processing capabilities of the APs, since the computations are now spread over the different APs in the user-centric network.

## V. DISTRIBUTED MULTI-USER RC

The proposed DUCERC algorithm as discussed in Section IV, is operating separately for each UE $k$ in the corresponding user-centric network $\mathcal{M}_k$. Since an AP $l$ is typically part of several user-centric networks, i.e., one for each UE $\tilde{k} \in \mathcal{D}_l$, it then obtains channels estimates for all $\tilde{k} \in \mathcal{D}_l$. These channel estimates provide an instantaneous estimate of the interference, as present in the expression of the receive combiner $\mathbf{w}_k^t$ in (18), whereas $\overline{\mathbf{R}}_{\tilde{k}}^{\mathcal{M}_k}$ in the expression of $\mathbf{v}_k^t$ in (16) only gives information on the interference averaged over all coherence blocks. The expression for (18) can be written using the quantities defined in Section III. To this end, the following quantity is defined

$$\mathbf{R}_{\tilde{k}}^{\mathcal{M}_k} = \mathbf{E}_{\tilde{k}}^{\mathcal{M}_k} \mathbf{R}_{\tilde{k}} \mathbf{E}_{\tilde{k}}^{\mathcal{M}_k H} \tag{74}$$

which possibly contains zero-columns and rows if some APs that serve UE $k$ do not serve UE $\tilde{k}$. So the proposed procedure to estimate $\mathbf{R}_{\tilde{k}}$ automatically results in an estimate for $\mathbf{R}_{\tilde{k}}^{\mathcal{M}_k}$. The following quantities can be similarly defined:

$$\begin{aligned} \mathbf{Q}_{\tilde{k}}^{\mathcal{M}_k,B} &= \mathbf{E}_{\tilde{k}}^{\mathcal{M}_k} \mathbf{Q}_{\tilde{k}}^{B}, \ \mathbf{X}_{\tilde{k}}^{\mathcal{M}_k,B} = \mathbf{E}_{\tilde{k}}^{\mathcal{M}_k} \mathbf{X}_{\tilde{k}}^{B}, \\ \mathbb{Q}_{\tilde{k}}^{\mathcal{M}_k,L} &= \mathbf{E}_{\tilde{k}}^{\mathcal{M}_k} \mathbb{Q}_{\tilde{k}}^{L}, \ \dot{\mathbb{Q}}_{\tilde{k}}^{\mathcal{M}_k} = \mathbf{E}_{\tilde{k}}^{\mathcal{M}_k} \dot{\mathbb{Q}}_{\tilde{k}}. \end{aligned} \tag{75}$$

The user-centric receive combiner $\mathbf{w}_k^t$ can then be written as provided in (76) shown at the bottom of the next page. Here it is again assumed that $\mathbf{M}_k$ is block diagonal with diagonal

[8] Note that these matrices are Hermitian symmetric, so it suffices to only compute the upper (or) lower triangular block via in-network sums, which will decrease the communication even further.

elements

$$\mathbf{M}_{kl} = \mathbf{R}_{all_k l} - \sum_{\tilde{k} \in \mathcal{D}_l} \left( \mathbb{Q}_{\tilde{k}l}^{\mathcal{M}_k, L} \mathbb{\Sigma}_{\tilde{k}}^{L} \mathbb{Q}_{\tilde{k}l}^{\mathcal{M}_k, L^H} + \mathbb{Q}_{\tilde{k}l}^{\mathcal{M}_k, B} \mathbb{\Sigma}_{\tilde{k}l}^{B} \mathbb{Q}_{\tilde{k}l}^{\mathcal{M}_k, B^H} \right) \tag{77}$$

that can be computed locally at each AP, since it has access to all these quantities. The following quantity and its $l$th block row is also defined in (76):

$$\mathbf{N}_k = [\mathbf{Q}_1^{\mathcal{M}_k, B} \mathbf{z}_1^{t,B} \ldots \mathbf{Q}_{K_k}^{\mathcal{M}_k, B} \mathbf{z}_{K_k}^{t,B} \; \dot{\mathbb{Q}}_1^{\mathcal{M}_k} \ldots \dot{\mathbb{Q}}_{K_k}^{\mathcal{M}_k}] \tag{78}$$

$$[\mathbf{N}_k]_l = [\mathbb{Q}_{1^\frown l}^{B} \mathbf{z}_{1^\frown l}^{t,B} \ldots \mathbb{Q}_{K_k l}^{B} \mathbf{z}_{K_k l}^{t,B} \; \dot{\mathbb{Q}}_{1^\frown l} \ldots \dot{\mathbb{Q}}_{K_k l}] \tag{79}$$

where $\dot{\mathbb{Q}}_{\tilde{k}l}$ and $\mathbf{Q}_{\tilde{k}l}^{B} \mathbf{z}_{\tilde{k}l}^{t,B}$ are set to zero if $\tilde{k} \notin \mathcal{D}_l$.

Note that $\mathbf{S}_k \in \mathbb{C}^{K_k(1+R^L) \times K_k(1+R^L)}$ can then be computed using in-network sums as

$$\mathbf{S}_k = \sum_{l \in \mathcal{M}_k} \mathbf{\Psi}_k [\mathbf{N}_k]_l^H \mathbf{M}_{kl}^{-1} [\mathbf{N}_k]_l. \tag{80}$$

If an AP $l$ has access to $\mathbf{S}_k$, it can approximate the local version of the receive combiner $\mathbf{w}_{kl}^t$ as

$$\mathbf{M}_{kl}^{-1} [\mathbf{N}_k]_l \left( \mathbf{I}_{K_k(1+R^L)} + \mathbf{S}_k \right)^{-1} \begin{bmatrix} \mathbf{0}_{(k-1)(1+R^L)} \\ 1 \\ \mathbf{z}_k^{t,L} \\ \mathbf{0}_{(K_k-k)(1+R^L)} \end{bmatrix} \tag{81}$$

This receive combiner can be easily included in Algorithm 2 by replacing the second bullet in step 5 with the computation of the in-network sum of $\mathbf{S}_k$ and the third bullet with computing $\mathbf{w}_{kl}^t$ using (81). This increases the communication cost by a factor $K_k$ during RC. Intermediate receive combiners, where only a subset of the strongest interfering UEs are included in $\mathcal{P}_k$ can similarly be derived and will decrease the communication cost. As a limit, i.e., when $\mathcal{P}_k = \{k\}$, the filter $\mathbf{v}_k^t$ will again be obtained.

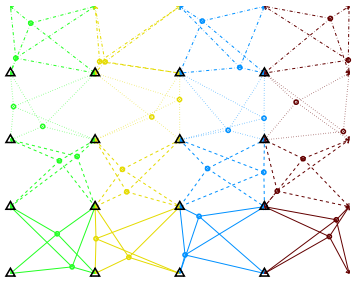

**FIGURE 4.** CFmMIMO setup with $L = 16$ and $K = 32$ and using the wrap-around technique.

## VI. SIMULATIONS

In this section, simulations for the centralized and distributed GEVD-based CE and RC are conducted to compare the effect of using different rank constraints and to investigate convergence properties. To this end, a scenario is simulated with $L = 16$ APs with $N = 16$ antennas arranged in a square grid of 300 m. The wrap-around technique is used to simulate an infinite network. Two UEs are randomly positioned in each square, such that $K = 32$. $\mathcal{M}_k$ is given by the four surrounding APs as indicated in Fig. 4 ($L_k = 4$). The transmit power is set to 100 mW and $\tau_p$ is set to 4. All provided results are averaged over 20 realizations.

The large-scale fading coefficient $\overline{\mathbf{G}}_k$ is simulated as a block diagonal matrix with $\overline{\mathbf{G}}_{kl}$ modeled as [41, Sec. 2.6]. The LoS component $\overline{\mathbf{h}}_k$ is modeled as [41, Sect. 1.3], with $||\overline{\mathbf{h}}_{kl}||^2 = \text{tr}\{\overline{\mathbf{G}}_{kl}\}$. The channels are then generated as

$$\mathbf{h}_k^t = \sqrt{1-\beta}\overline{\mathbf{h}}_k e^{j\varphi_k^t} + \sqrt{\beta}\mathbf{g}_k^t \tag{82}$$

where $\beta$ is a control parameter and is chosen such that $\text{tr}\{\overline{\mathbf{R}}_k\}$ is independent of $\beta$. Here $\beta = 0$ models only a LoS component, $\beta = 1$ models only a NLoS component, and $0 < \beta < 1$ models a combination of both components.

The performance measure used is a standard capacity lower bound [41] referred to as the achievable spectral efficiency

$$\begin{aligned}
\mathbf{w}_k^t \approx & \Bigg( \underbrace{\mathbf{R}_{all_k} - \sum_{\tilde{k} \in \mathcal{P}_k} \left( \mathbb{Q}_{\tilde{k}}^{\mathcal{M}_k, L} \mathbb{\Sigma}_{\tilde{k}}^{L} \mathbb{Q}_{\tilde{k}}^{\mathcal{M}_k, L^H} + \mathbf{Q}_{\tilde{k}}^{\mathcal{M}_k, B} \mathbf{\Sigma}_{\tilde{k}}^{B} \mathbf{Q}_{\tilde{k}}^{\mathcal{M}_k, B^H} \right)}_{\mathbf{M}_k} + \sum_{\tilde{k} \in \mathcal{P}_k} [\mathbf{Q}_{\tilde{k}}^{\mathcal{M}_k, B} \mathbf{z}_{\tilde{k}}^{t,B} \; \dot{\mathbb{Q}}_{\tilde{k}}^{\mathcal{M}_k}] \begin{bmatrix} 1 & \mathbf{z}_{\tilde{k}}^{t,L^H} \\ \mathbf{z}_{\tilde{k}}^{t,L} & \mathbf{z}_{\tilde{k}}^{t,L} \mathbf{z}_{\tilde{k}}^{t,L^H} + \mathbb{\Psi}_{\tilde{k}}^{L} \end{bmatrix} \\
& \times \begin{bmatrix} \mathbf{z}_{\tilde{k}}^{t,B^H} \mathbf{Q}_{\tilde{k}}^{\mathcal{M}_k, B^H} \\ \dot{\mathbb{Q}}_{\tilde{k}}^{\mathcal{M}_k H} \end{bmatrix} \Bigg)^{-1} [\mathbf{Q}_k^B \mathbf{z}_k^{t,B} \; \dot{\mathbb{Q}}_k] \begin{bmatrix} 1 \\ \mathbf{z}_k^{t,L} \end{bmatrix} \\
= & \mathbf{M}_k^{-1} \mathbf{N}_k \Bigg( \mathbf{I}_{K_k(1+R^L)} + \underbrace{\begin{bmatrix} \mathbf{I}_{K_k} & \text{blkdiag}\{\mathbf{z}_1^{t,L}, \ldots, \mathbf{z}_{K_k}^{t,L}\}^H \\ \text{blkdiag}\{\mathbf{z}_1^{t,L}, \ldots, \mathbf{z}_{K_k}^{t,L}\} & \text{blkdiag}\{\mathbf{z}_1^{t,L} \mathbf{z}_1^{t,L^H} + \mathbb{\Psi}_1^L, \ldots, \mathbf{z}_{K_k}^{t,L} \mathbf{z}_{K_k}^{t,L^H} + \mathbb{\Psi}_{K_k}^L\} \end{bmatrix}}_{\mathbf{\Psi}_k} \mathbf{N}_k \mathbf{M}_k^{-1} \mathbf{N}_k \Bigg)^{-1} \underbrace{\begin{bmatrix} \mathbf{0}_{(k-1)(1+R^L)} \\ 1 \\ \mathbf{z}_k^{t,L} \\ \mathbf{0}_{(K_k-k)(1+R^L)} \end{bmatrix}}_{\mathbf{S}_k}
\end{aligned} \tag{76}$$

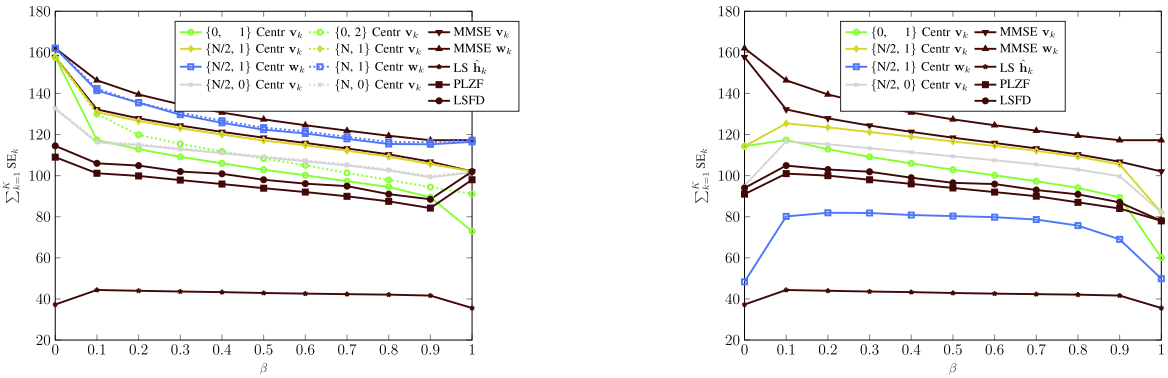


(a) $T = 10000$ (b) $T = 500$

**FIGURE 5.** Performance of proposed centralized rank $\{R^B, R^L\}$ GEVD-based RC and CE.

(SE) and is given by

$$\mathrm{SE}_k = \frac{\tau_u}{\tau_p + \tau_u} E\{\log_2\left(1 + \mathrm{SINR}_k^t\right)\} \text{ with } \mathrm{SINR}_k^t = \frac{|\mathbf{v}_k^{t\,H} \hat{\mathbf{h}}_k^t|^2}{\sum_{\tilde{k} \in \tilde{\mathcal{P}}_k} |\mathbf{v}_k^{t\,H} \hat{\mathbf{h}}_{\tilde{k}}^{\mathcal{M}_k t}|^2 + \mathbf{v}_k^{t\,H}\left(\sum_{\tilde{k} \in \mathcal{P}_k} \overline{\mathbf{C}}_{\tilde{k}}^{\mathcal{M}_k} + \overline{\mathbf{R}}_{\mathbf{nn}}^{\mathcal{M}_k}\right)\mathbf{v}_k^t} \tag{83}$$

where the channel estimates are given by the optimal MMSE-based channel estimates. Note that the MMSE-based receive combiner $\overline{\mathbf{w}}_k^t$ maximizes $\mathrm{SINR}_k^t$.

Finally three reference methods are provided. The LS method uses the channel estimate $\frac{1}{\sqrt{\tau_p}} \mathbf{y}_{\tau_k}^{\mathcal{M}_k t}$ and uses MR combining for the RC. The local partial zero-forcing (LPZF) combiner [32] and large-scale fading decoding (LSFD) combiner [13], [29] use local channel estimation and receive combining. Note that correlation between APs in case of LoS channels is not exploited.

### A. RESULTS FOR CENTRALIZED GEVD-BASED CE AND RC

The CE performance depends on the estimation of $\mathbf{R}_{\tau_k}$ and $\mathbf{R}_{all_k}$ using the signals obtained during the pilot phase. MMSE-based CE assumes perfect knowledge of these matrices, including perfect knowledge of $\mathbf{R}_k$. The matrices are better estimated whenever the number of coherence blocks $T$ increases and the RC will also improve with better channel estimates. Therefore, the sum-SE for 2 cases, i.e., $T = 10000$ and $T = 500$, is provided in Fig. 5 for different values of $\beta$ and for different combinations of $\{R^B, R^L\}$.

For $T = 1000$, it is observed that estimating $\mathbf{w}_k$ by using a rank $\{N, 1\}$ GEVD achieves the best performance and that its performance is close to the performance of the MMSE-based receive combiner $\overline{\mathbf{w}}_k$. Similarly, estimating $\mathbf{v}_k$ by using a rank $\{N, 1\}$ GEVD also achieves a performance very close to the performance of the MMSE-based receive combiner $\overline{\mathbf{v}}_k$. This shows that approximating $\mathbf{R}_{\tau_k} - \tau_p \mathbb{Q}_k^L \mathbb{\Sigma}_k^L \mathbb{Q}_k^{L\,H}$, $\mathbf{B}_k$ and $\mathbf{M}_k$ as block diagonal matrices is valid with the used channel estimates. Rank approximations with $R^B = 0$ work best for small $\beta$ and increasing $R^L$ gives better performance since $\mathbf{R}_k$ can be better approximated. Rank approximation with $R^L = 0$ is also performing well but including $R^L$ has clearly some benefits for channels with a LoS component. Using $R^B = N/2$ instead of $N$ only reduces the performance slightly. This is because most of the generalized eigenvalues in $\mathbb{\Sigma}_k^B$ are close to zero (or negative and thereby set to zero using $[\cdot]_0$), so setting $R^B$ to $N/2$ gives good results and saves some complexity in the computation of the GEVD.

The proposed centralized GEVD-based RC and CE also outperforms the reference methods (LS, PLZF, LSFD) under different settings of $\{R^B, R^L\}$. This can be explained because correlation between APs in case of LoS channels is not exploited in this method and the contributions of the different APs are optimally combined using the network sums. The PLZF and LSFD method perform similar to the MMSE-based receive combiner $\overline{\mathbf{v}}_k$ for $\beta = 1$, showing that they are valid methods when there is no correlation between the different APs, for which they were also developed initially.

Generally, a decrease in sum-SE is observed over all methods when $\beta$ increases, i.e. the correlation between the different APs is traded for stronger correlation between the antennas locally. Using and optimally exploiting the diversity obtained from APs located in different positions of the network, has thus an advantageous effect on the total network performance, especially for UEs experiencing channels with low SINR conditions. This is one of the key enablers to opt for CFmMIMO networks, compared to cellular networks [9].

For $T = 500$, similar observations can be made. The only exception is that the performance of estimating $\mathbf{w}_k$ by using a rank $\{N/2, 1\}$ GEVD has dropped drastically. This can be explained by the fact that some channels with low SINR are poorly estimated, but their channel estimates are still included in $\mathbf{w}_k$. However, when working with smaller values for $T$, it is advised to use the receive combiner $\mathbf{v}_k$, which has also a lower communication cost in DUCERC.

### B. RESULTS FOR RANK $\{R^B, R^L\}$ GEVD-BASED DUCERC

In this section, the convergence of rank $\{R^B, R^L\}$ GEVD-based DUCERC is investigated and compared to the centralized

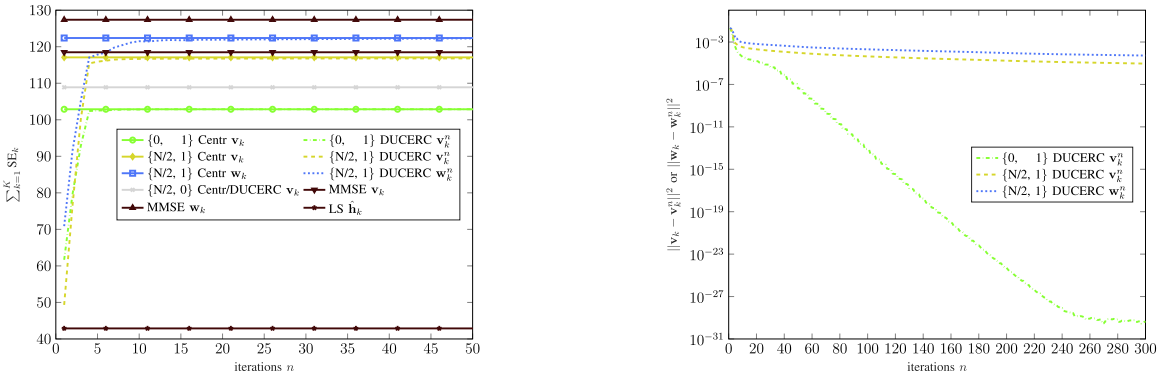


(a) Performance (b) Convergence

**FIGURE 6.** Performance and convergence of rank $\{R^B, R^L\}$ DUCERC for $T = 10000$ and $\beta = 0.5$.

**TABLE 1.** Performance of the Proposed Centralized Rank $\{R^B, R^L\}$ GEVD-Based RC and CE for $\beta = 0.5$, $T = 10\,000$ and a Varying Number of AP and Antennas (Total Number of Antennas Remains Constant)

| $\sum_{k=1}^K \mathrm{SE}_k$ | MMSE $\overline{\mathbf{w}}_k$ | $\{N/2, 1\}$ Centr $\mathbf{w}_k$ | MMSE $\overline{\mathbf{v}}_k$ | $\{N/2, 1\}$ Centr $\mathbf{v}_k$ | PLZF | LS |
|---|---|---|---|---|---|---|
| $L = 16, N = 16$ | 127.4 | 123.4 | 118.5 | 117.1 | 93.9 | 42.9 |
| $L = 32, N = 8$ | 174.7 | 169.5 | 168.9 | 165.2 | 140.8 | 82.5 |
| $L = 64, N = 4$ | 235.0 | 228.6 | 225.3 | 220.4 | 197.6 | 130.1 |

performance. The results for different iterations of DUCERC are provided in Fig. 6 and this for both the sum-SE as well as for the MSE-difference between the centralized and the distributed solution. $T$ and $\beta$ are set to 10000 and 0.5 respectively.

Looking at the achieved performance, it is observed that the DUCERC algorithm converges to a value similar to that of the centralized algorithm, and this already after 20 iterations. However, from the convergence figure, it is clear that there is only convergence to the machine precision when $R^B = 0$. When $R^B \neq 0$ this is no longer the case (as pointed out in Section IV-B), but the distributed filters are still achieving similar performance.

### C. RESULTS FOR CENTRALIZED GEVD-BASED CE AND RC WITH VARYING NUMBER OF APS/ANTENNAS

In this section, the performance of the proposed centralized rank $\{R^B, R^L\}$ GEVD-based RC and CE is evaluated when the number of APs and antennas is varied, while keeping the total number of antennas $LN = 256$ and UEs $K = 32$ the same as described supra. The area is also kept constant and the APs are positioned similar to a 16-QAM, 32-QAM and 64-QAM constellation diagram. The results for $\beta = 0.5$ and $T = 10000$ are provided in Table 1.

As generally observed in CFmMIMO [9], densifying the network with more APs has a beneficial impact on the performance. UEs with low SINR conditions benefit most from having many APs, since they get a higher probability of being close to an AP. UEs with already good SINR conditions achieve roughly the same SE even when having fewer multi-antenna APs. The same trend can be observed in the proposed methods, where the sum-SE scales almost linearly with the number of AP $L$ in the considered setup. The difference between the centralized MMSE methods and the proposed methods become larger when $L$ increases and $N$ decreases, which can be attributed to the bigger approximation error made when only considering a local rank $R^B = N/2$ approximation.

## VII. CONCLUSION

In this paper, a novel channel covariance estimator has been presented for user-centric CFmMIMO channels satisfying a general Rician fading model, i.e., with both LoS and NLoS components. The LoS component introduces correlation between the channels at different APs that can be exploited to improve the CE and in a later stage the RC. The proposed methods perform CE using GEVDs of two covariances that are estimated from the available UL data. The transmitted signals can then be obtained by processing the local antenna signals, together with $R^L$ compressed versions of all the antenna signals of all the APs serving the UE. To make the proposed method scalable, the DUCERC algorithm has been presented, which reduces the required communications between the APs to a minimum and relies on in-network sums that can be accomplished whenever the APs can be arranged into a tree-topology. All the computations are then distributed over the different APs. Simulations have shown that the performance of the proposed GEVD-based centralized and distributed CE and RC is close to the performance of optimal MMSE-based CE and RC with perfect CSI. Extending the current framework to more general fading models, e.g., the Kronecker product structure in the jointly-correlated

Weichselberger model with multi-antenna users [49], will be the topic of future research. Such models do not yet fit in the proposed structures of Section III.

## APPENDIX A
## PROOF OF (55)

*Proof:* Start by writing $\mathbf{R}_{\tau_k}^{-1}$ using the matrix inversion lemma:

$$\mathbf{R}_{\tau_k}^{-1} = \left( \underbrace{\left(\mathbf{R}_{\tau_k} - \tau_p \mathbb{Q}_k^L \mathbb{\Sigma}_k^L \mathbb{Q}_k^L\right)}_{\mathbf{A}} + \tau_p \mathbb{Q}_k^L \mathbb{\Sigma}_k^L \mathbb{Q}_k^L \right)^{-1}$$
$$= \mathbf{A}^{-1} - \mathbf{A}^{-1}\mathbb{Q}_k^L \left( \left(\tau_p \mathbb{\Sigma}_k^L\right)^{-1} + \mathbb{Q}_k^{L^H} \mathbf{A}^{-1} \mathbb{Q}_k^L \right)^{-1} \mathbb{Q}_k^{L^H} \mathbf{A}^{-1}. \tag{84}$$

Also note that

$$\mathbf{A}^{-1}\mathbb{Q}_k^L = \mathbf{R}_{\tau_k}^{-1}\mathbb{Q}_k^L \left(\mathbf{I}_{R^L} - \tau_p \mathbb{\Sigma}_k^L \mathbb{Q}_k^{L^H} \mathbf{R}_{\tau_k}^{-1} \mathbb{Q}_k^L\right)^{-1}$$
$$= \mathbf{R}_{\tau_k}^{-1}\mathbb{Q}_k^L \left(\mathbf{I}_{R^L} - \tau_p \mathbb{\Sigma}_k^L\right)^{-1} \tag{85}$$

and

$$\mathbb{Q}_k^{L^H} \mathbf{A}^{-1} \mathbb{Q}_k^L = \left(\mathbf{I}_{R^L} - \tau_p \mathbb{\Sigma}_k^L\right)^{-1} \tag{86}$$

which uses the fact that the columns in $\mathbb{Q}_k^L$ are normalized such that $\mathbb{Q}_k^{L^H} \mathbf{R}_{\tau_k}^{-1} \mathbb{Q}_k^L = \mathbb{Q}_k^{L^H} \mathbb{X}_k^L = \mathbf{I}_{R^L}$.

By substituting (85) and (86) in (84) and after some manipulations, the following identity is obtained:

$$\mathbf{R}_{\tau_k}^{-1} = \mathbf{A}^{-1} - \mathbf{R}_{\tau_k}^{-1}\mathbb{Q}_k^L \tau_p \mathbb{\Sigma}_k^L \left(\mathbf{I}_{R^L} - \tau_p \mathbb{\Sigma}_k^L\right)^{-1} \mathbb{Q}_k^{L^H} \mathbf{R}_{\tau_k}^{-1}. \tag{87}$$

Finally, by using

$$\begin{aligned} \mathbf{A}^{-1}\mathbb{Q}_k^B &\approx \mathbb{X}_k^B \\ \mathbf{R}_{\tau_k}^{-1}\mathbb{Q}_k^L &= \mathbb{X}_k^L \end{aligned} \tag{88}$$

and

$$\mathbf{R}_{\tau_k}^{-1}\mathbb{Q}_k^B \approx \mathbb{X}_k^B - \mathbb{X}_k^L \tau_p \mathbb{\Sigma}_k^L \left(\mathbf{I}_{R^L} - \tau_p \mathbb{\Sigma}_k^L\right)^{-1} \mathbb{X}_k^{L^H} \mathbb{Q}_k^B \tag{89}$$

in (55) and after rearranging, the desired result is obtained. ■

## APPENDIX B
## PROOF OF THEOREM IV.1

In this section, the convergence proof for the simplified (virtual) algorithm (VA) provided in Algorithm 3 is given. This is a simplified version of steps 1–4 and 6 of Algorithm 2 whenever the block diagonal quantities are kept constant during the algorithm and when the covariance matrices $\tilde{\mathbf{R}}_{\tau_k q}$ and $\tilde{\mathbf{R}}_{all_k q}$ are perfectly estimated. Theorem IV.1 will be proven for this algorithm, by linking Algorithm 3 to another VA for which convergence can be proven.

Before introducing the VA, it has to be marked that instead of performing a joint diagonalization as in (32) and computing $\mathbb{X}_k^L$ as $\mathbf{R}_{\tau_k}^{-1}\mathbb{Q}_k^L$, it is also possible to compute $\mathbb{X}_k^L$ directly from:

$$\mathbb{X}_k^L = \arg\min_{\mathbb{X}_k} \mathbb{X}_k^H (\mathbf{R}_{all_k} + (\tau_p - 1)\mathbf{R}_k^{B,\bar{n}})\mathbb{X}_k$$
$$s.t.\ \mathbb{X}_k^H \mathbf{R}_{\tau_k} \mathbb{X}_k = \mathbf{I}_{R^L} \tag{94}$$

where $\mathbb{\Sigma}_{all_k}^L = \mathbb{X}_k^{L^H} \mathbf{R}_{all_k} \mathbb{X}_k^L$. Note that $\mathbb{X}_k^L$ (without iteration index $n$) will be used to denote optimal solutions. $\mathbb{Q}_k^L$ can then be found as $\mathbf{R}_{\tau_k}\mathbb{X}_k^L$.

A VA that searches for the $R^L$ generalized eigenvectors of $\{(\mathbf{R}_{all_k} + (\tau_p - 1)\mathbf{R}_k^{B,\bar{n}}), \mathbf{R}_{\tau_k}\}$ corresponding to the smallest generalized eigenvalues is provided in Algorithm 4. It is an alternating optimization algorithm with the following convergence property:

*Theorem B.1:* For any initialization of Algorithm 4, $\lim_{n\to\infty} \mathbb{X}_k^{L,n+1}$ exists, i.e., Algorithm 4 converges. Furthermore $\mathbb{X}_k^{L,n+1}$ converges to the same solution as (94), i.e., $\lim_{n\to\infty} \mathbb{X}_k^{L,n+1} = \mathbb{X}_k^L$. Moreover $\lim_{n\to\infty} \mathbb{\Sigma}_{all_k}^{L,n} = \mathbb{\Sigma}_{all_k}^L$.

*Proof:* The proof can be constructed similarly to the proof of Theorem II in [38], albeit that there are a few key differences to be pointed out for completeness. Firstly, everywhere

**Algorithm 3:** Simplified Version of Algorithm 2.

1: Set $n \leftarrow 0$, $q \leftarrow 1$ and initialize $\mathbf{F}_{kl}^0\ \forall l \in \mathcal{M}_k$ randomly.

2: Construct the AP-specific compression matrix $\check{\mathbf{J}}_{kq}^n$

$$\tilde{\mathbf{J}}_{kq}^n = \begin{bmatrix} \mathbf{0}_{(q-1)N\times N} & \mathbf{F}_{k,<q}^n \\ \mathbf{I}_N & \mathbf{0}_{N\times R^L} \\ \mathbf{0}_{(L_k-q)N\times N} & \mathbf{F}_{k,>q}^n \end{bmatrix} \tag{90}$$

with $\mathbf{F}_{k,<q}^n = [\mathbf{F}_{k1}^{n^H} \ldots \mathbf{F}_{k,q-1}^{n^H}]^H$, $\mathbf{F}_{k,>q}^n = [\mathbf{F}_{k,q+1}^{n^H} \cdots \mathbf{F}_{kL_k}^{n^H}]^H$.

3: AP $q$ estimates $\tilde{\mathbf{R}}_{all_k q}$, $\tilde{\mathbf{R}}_{all_k q}^{B,n}$ and $\tilde{\mathbf{R}}_{\tau_k q}$ perfectly as

$$\begin{aligned} \tilde{\mathbf{R}}_{all_k q} &= \tilde{\mathbf{J}}_{kq}^{n^H} \mathbf{R}_{all_k} \tilde{\mathbf{J}}_{kq}^n \\ \tilde{\mathbf{R}}_{kq}^{B,\bar{n}} &= \tilde{\mathbf{J}}_{kq}^{n^H} \mathbf{R}_k^{B,\bar{n}} \tilde{\mathbf{J}}_{kq}^n \\ \tilde{\mathbf{R}}_{\tau_k q} &= \tilde{\mathbf{J}}_{kq}^{n^H} \mathbf{R}_{\tau_k} \tilde{\mathbf{J}}_{kq}^n. \end{aligned} \tag{91}$$

4: Compute $\tilde{\mathbb{Q}}_{kq}^{L,n+1}$, $\mathbb{\Sigma}_{kq}^{L,n+1}$, $\mathbb{\Sigma}_{all_k q}^{L,n+1}$, $\tilde{\mathbb{X}}_{kq}^{L,n+1}$ and $\tilde{\mathbf{R}}_{kq}^{L,n+1}$ from the GEVD of $\{\tilde{\mathbf{R}}_{\tau_k q}, \tilde{\mathbf{R}}_{all_k q} + (\tau_p - 1)\tilde{\mathbf{R}}_{kq}^{B,n}\}$ similar as in (42)–(45).

5: Update the compression matrix as

$$\mathbf{F}_{kq}^{n+1} = \mathbb{X}_{kq}^{L,n+1} \left(\mathbb{X}_{k,-q}^{L,n+1}\right)^{-1} \tag{92}$$

which is equivalent to

$$\mathbf{F}_k^{n+1} = \tilde{\mathbf{J}}_k^n \tilde{\mathbb{X}}_{kq}^{L,n+1} \left(\mathbb{X}_{k,-q}^{L,n+1}\right)^{-1}. \tag{93}$$

6: $n \leftarrow n+1$ and $q \leftarrow (q \mod L_k) + 1$ and return to step 2.

**TABLE 2. Overview of Main Mathematical Symbols. Quantities With (∗) are Also Present Without ˘ to Denote Data-Based Estimates of the True Quantities**

| Symbol | Meaning |
|---|---|
| $\mathcal{M}_k$ | $\{l \vert \text{AP } l \text{ observes UE } k\} = \{1, ..., L_k\}$ |
| $\mathcal{D}_l$ | $\{k \vert l \in \mathcal{M}_k\}$ |
| $\mathcal{P}_k$ | $\{\tilde{k} \vert \mathcal{M}_{\tilde{k}} \cap \mathcal{M}_k \neq \emptyset\} = \{1, ..., K_k\}$ |
| $\tilde{\mathcal{P}}_k$ | $\mathcal{P}_k \setminus \{k\}$ |
| $\mathbf{y}_l^t$ | Local antenna signal of AP $l$ in coherence block $t$ |
| $\mathbf{y}^{\mathcal{M}_k t}$ | User-centric antenna signal $\mathbf{y}^{\mathcal{M}_k t} = [\mathbf{y}_1^{t\,H} \ ... \ \mathbf{y}_{L_k}^{t\,H}]^H$ in coherence block $t$ |
| $\mathbf{h}_{kl}^t$ | Channel between UE $k$ and AP $l$ in coherence block $t$ |
| $\mathbf{h}_{\bar{k}}^{\mathcal{M}_k t}$ | Channel between UE $\bar{k}$ and all AP in $\mathcal{M}_k$ in coherence block $t$ |
| $\mathbf{h}_k^t$ | Same as $\mathbf{h}_k^{\mathcal{M}_k t}$ |
| $\overline{\mathbf{R}}_k(*)$ | True channel covariance matrix $E\{\mathbf{h}_k^t \mathbf{h}_k^{t\,H}\}$ |
| $\mathbf{y}_{all_k}^{\mathcal{M}_k t}[p]$ | Despreaded received user-centric antenna signal with training sequence $p$ in coherence block $t$ |
| $\mathbf{y}_{\tau_k}^{\mathcal{M}_k t}$ | Despreaded received user-centric antenna signal with the training sequence of UE $k$ in coherence block $t$ |
| $\overline{\mathbf{R}}_{\tau_k}^{\mathcal{M}_k}(*)$ | $E\{\mathbf{y}_{\tau_k}^{\mathcal{M}_k t} \mathbf{y}_{\tau_k}^{\mathcal{M}_k t\,H}\}$ |
| $\overline{\mathbf{R}}_{all_k}^{\mathcal{M}_k}(*)$ | $E\{\frac{1}{\tau_p}\sum_{p=1}^{\tau_p} \mathbf{y}_{all_k}^{\mathcal{M}_k t}[p] \mathbf{y}_{all_k}^{\mathcal{M}_k t\,H}[p]\}$ |
| $\overline{\mathbf{W}}_k(*)$ | True MMSE-based CE filter |
| $\hat{\overline{\mathbf{h}}}_k^t(*)$ | True MMSE-based channel estimate given by $\overline{\mathbf{W}}_k^H \mathbf{y}_{\tau_k}^{\mathcal{M}_k t}$ in coherence block $t$ |
| $\overline{\mathbf{C}}_k(*)$ | True estimation error covariance matrix |
| $\overline{\mathbf{v}}_k^t(*)$ | True MMSE-based RC $\mathbf{v}_k^t = [\mathbf{v}_{k1}^{t\,H} \ ... \ \mathbf{v}_{kL_k}^{t\,H}]^H$ in coherence block $t$ |
| $\overline{\mathbf{w}}_k^t(*)$ | True multi-user MMSE-based RC $\mathbf{w}_k^t = [\mathbf{w}_{k1}^{t\,H} \ ... \ \mathbf{w}_{kL_k}^{t\,H}]^H$ in coherence block $t$ |
| $\overline{\mathbf{q}}_k^B \overline{\mathbf{\Sigma}}_k^B \overline{\mathbf{q}}_k^{B\,H}(*)$ | Low rank approximation of the block diagonal part $\overline{\mathbf{R}}_k^B$ (NLoS) in $\overline{\mathbf{R}}_k$ |
| $\overline{\mathbb{Q}}_k^L \overline{\mathbb{\Sigma}}_k^L \overline{\mathbb{Q}}_k^{L\,H}(*)$ | Low rank approximation of the LoS-component $\overline{\mathbf{R}}_k^L$ in $\overline{\mathbf{R}}_k$ |
| $\mathbf{z}_k^{t,B}$ | Compressed local antenna signal of AP $l$ in coherence block $t$ given by $\sqrt{\tau_p}\mathbf{\Sigma}_k^B \mathbf{X}_k^{B\,H} \mathbf{y}_{\tau_k}^{\mathcal{M}_k t}$ |
| $\mathbf{z}_k^{t,L}$ | Compressed user-centric antenna signal for APs in $\mathcal{M}_k$ given by $\sqrt{\tau_p}\mathbb{\Sigma}_k^L \mathbb{X}_k^{L\,H} \mathbf{y}_{\tau_k}^{\mathcal{M}_k t}$ |
| $\mathbf{F}_{kl}^n$ | Compression matrix to compress $\mathbf{y}_l^t$ to obtain $\chi_{kl}^t$ for the DUCERC algorithm in iteration $n$ |
| $\alpha_k^t, \beta_k^t, \mathbf{\Gamma}_k$ | Parameters obtained using in-network sums for the DUCERC algorithm |

in the algorithm, $\mathbf{R}_{\mathbf{yy}}$ and $\mathbf{R}_{\mathbf{nn}}$ have to be replaced with $(\mathbf{R}_{all_k} + (\tau_p - 1)\mathbf{R}_k^{B,\bar{n}})$ and $\mathbf{R}_{\tau_k}$ respectively. Secondly, instead of searching for the $R^L$ generalized eigenvectors corresponding the the smallest generalized eigenvalues, a maximization in (98) is used to obtain the $R^L$ generalized eigenvectors corresponding the the largest generalized eigenvalues. However, the proof is still valid if the words 'max', 'increase' and '$\geq$' (e.g., in $f(\underline{\mathbb{X}}^{i+1}) \geq f(\underline{\mathbb{X}}^i)$) are merely replaced with 'min', 'decrease' and '$\leq$'. Finally, the algorithm in [38] defines the AP-specific compression matrix $\mathbf{J}_{kq}^n$ as

$$\mathbf{J}_{kq}^n = \begin{bmatrix} \mathbf{0} & \text{blkdiag}\{\underline{\mathbb{X}}_{k1}^n \ldots \underline{\mathbb{X}}_{k,q-1}^n\} & \mathbf{0}_{(q-1)N \times (L_k - q)N} \\ \mathbf{I}_N & \mathbf{0}_{N \times (q-1)N} & \mathbf{0}_{N \times (L_k - q)N} \\ \mathbf{0} & \mathbf{0}_{(L_k - q)N \times (q-1)N} & \text{blkdiag}\{\underline{\mathbb{X}}_{k,q+1}^n \ldots \underline{\mathbb{X}}_{kL_k}^n\} \end{bmatrix} \tag{95}$$

whereas here the compression matrix is defined as in (96). This has no further impact on the provided arguments in the proof, so the proof is also valid for the compression matrix in (96). ■

**Algorithm 4:** VA to Estimate the $R^L$ Generalized Eigenvectors.

1: Set $n \leftarrow 0$, $q \leftarrow 1$ and initialize $\underline{\mathbb{X}}_{kl}^{L,0}$ $\forall l \in \mathcal{M}_k$ randomly.
2: Construct the AP-specific compression matrix $\breve{\mathbf{J}}_{kq}^n$

$$\breve{\mathbf{J}}_{kq}^n = \begin{bmatrix} \mathbf{0}_{(q-1)N \times N} & \underline{\mathbb{X}}_{k,<q}^n \\ \mathbf{I}_N & \mathbf{0}_{N \times R^L} \\ \mathbf{0}_{(L_k - q)N \times N} & \underline{\mathbb{X}}_{k,>q}^n \end{bmatrix}. \tag{96}$$

3: AP $q$ estimates $\breve{\mathbf{R}}_{all_k q}$, $\breve{\mathbf{R}}_{all_k q}^{B,n}$ and $\breve{\mathbf{R}}_{\tau_k q}$ perfectly as

$$\begin{aligned} \breve{\mathbf{R}}_{all_k q} &= \breve{\mathbf{J}}_{kq}^{n\,H} \mathbf{R}_{all_k} \breve{\mathbf{J}}_{kq}^n \\ \breve{\mathbf{R}}_{kq}^{B,\bar{n}} &= \breve{\mathbf{J}}_{kq}^{n\,H} \mathbf{R}_k^{B,\bar{n}} \breve{\mathbf{J}}_{kq}^n \\ \breve{\mathbf{R}}_{\tau_k q} &= \breve{\mathbf{J}}_{kq}^{n\,H} \mathbf{R}_{\tau_k} \breve{\mathbf{J}}_{kq}^n. \end{aligned} \tag{97}$$

4: Compute $\breve{\underline{\mathbb{X}}}_{kq}^{L,n+1}$ as

$$\begin{aligned} \breve{\underline{\mathbb{X}}}_{kq}^{L,n+1} = \arg\min_{\breve{\underline{\mathbb{X}}}_{kq}} & \ \breve{\underline{\mathbb{X}}}_{kq}^H \left(\breve{\mathbf{R}}_{all_k} + (\tau_p - 1)\breve{\mathbf{R}}_{kq}^{B,\bar{n}}\right) \breve{\underline{\mathbb{X}}}_{kq} \\ s.t. & \ \breve{\underline{\mathbb{X}}}_{kq}^H \breve{\mathbf{R}}_{\tau_k} \breve{\underline{\mathbb{X}}}_{kq}. \end{aligned} \tag{98}$$

5: $\underline{\mathbb{X}}_k^{L,n+1} = \breve{\mathbf{J}}_{kq}^n \breve{\underline{\mathbb{X}}}_{kq}^{L,n+1}$ and
$\underline{\mathbb{\Sigma}}_{all_k}^{L,n+1} = \breve{\underline{\mathbb{X}}}_{kq}^{L,n+1\,H} (\breve{\mathbf{R}}_{all_k} + (\tau_p - 1)\breve{\mathbf{R}}_{kq}^{B,\bar{n}}) \breve{\underline{\mathbb{X}}}_{kq}^{L,n+1}$.
6: $n \leftarrow n + 1$ and $q \leftarrow (q \mod L_k) + 1$ and return to step 2.

The next lemma links Algorithms 3 to 4.

*Lemma B.2:* If Algorithms 3 and 4 are initialized with the same matrix, i.e., $\underline{\mathbb{X}}_{kl}^{L,0} = \mathbf{F}_{kl}^{L,0}$ $\forall l$, then Algorithm 3 will produce the sequence

$$\mathbf{F}_k^n = \underline{\mathbb{X}}_k^{L,n} \left(\mathbb{X}_{k,-q}^{L,n}\right)^{-1} \quad \forall n \in \mathbb{N}_0 \tag{99}$$

$$\tilde{\underline{\mathbb{\Sigma}}}_{all_k q}^{L,n} = \underline{\mathbb{\Sigma}}_{all_k}^{L,n} \qquad \forall n \in \mathbb{N}_0. \tag{100}$$

Using (93) and Theorem B.2, this also implies that

$$\lim_{n \to \infty} \tilde{\mathbf{J}}_{kq}^n \tilde{\underline{\mathbb{X}}}_{kq}^{L,n} = \lim_{n \to \infty} \mathbf{F}_k^n \mathbb{X}_{k,-q}^{L,n} = \lim_{n \to \infty} \underline{\mathbb{X}}_k^{L,n} = \mathbb{X}_k^L. \tag{101}$$

*Proof:* By defining $\mathbb{X}_{k,-q}^{L,0} = \mathbf{I}_{R^L}$, the lemma holds for $n = 0$. The lemma will be proven using an inductive argument. To this end, it is assumed that the lemma holds up to iteration $n$ with updating AP $\bar{q}$, i.e., $\mathbf{F}_k^n = \underline{\mathbb{X}}_k^n (\mathbb{X}_{k,-\bar{q}}^{L,n})^{-1}$, from which it will be shown that $\mathbf{F}_k^{n+1} = \underline{\mathbb{X}}_k^{n+1} (\mathbb{X}_{k,-q}^{L,n+1})^{-1}$ with $q$ the next updating node. The following relation follows directly from

(90) and (96):

$$\tilde{\mathbf{J}}_{kq}^{n} = \check{\mathbf{J}}_{kq}^{n} \begin{bmatrix} \mathbf{I}_N & \mathbf{0}_{N\times R^L} \\ \mathbf{0}_{R^L\times N} & \left(\mathbb{X}_{k,-\bar{q}}^{L,n}\right)^{-1} \end{bmatrix}. \tag{102}$$

Since $\tilde{\mathbb{X}}_{kq}^{n+1}$ in step 2 of Algorithm 3 is the optimal solution of

$$\begin{aligned} \tilde{\mathbb{X}}_{kq}^{L,n+1} = \arg\min_{\tilde{\mathbb{X}}_{kq}} \; & \tilde{\mathbb{X}}_{kq}^{H} \tilde{\mathbf{J}}_{kq}^{nH} \left(\mathbf{R}_{all_k} + (\tau_p - 1)\mathbf{R}_{kq}^{B,\bar{n}}\right) \tilde{\mathbf{J}}_{kq}^{n} \tilde{\mathbb{X}}_{kq} \\ & s.t. \; \tilde{\mathbb{X}}_{kq}^{H} \tilde{\mathbf{J}}_{kq}^{nH} \mathbf{R}_{\tau_k} \tilde{\mathbf{J}}_{kq}^{n} \tilde{\mathbb{X}}_{kq} \end{aligned} \tag{103}$$

and $\check{\mathbb{X}}_{kq}^{L,n+1}$ is given by (98), the optimal solutions can be found using (102). The optimal solutions are then equal up to a certain matrix multiplication

$$\tilde{\mathbb{X}}_{kq}^{n+1} = \begin{bmatrix} \mathbf{I}_N & \mathbf{0}_{N\times R^L} \\ \mathbf{0}_{R^L\times N} & \mathbb{X}_{k,-\bar{q}}^{L,n} \end{bmatrix} \check{\mathbb{X}}_{kq}^{n+1} \tag{104}$$

where the invertibility of $\mathbb{X}_{k,-q}^{L,n}$ is used.

As a consequence, $\mathbf{F}_k^{n+1}$ can be written as

$$\begin{aligned} \mathbf{F}_k^{n+1} &= \tilde{\mathbf{J}}_k^{n} \tilde{\mathbb{X}}_{kq}^{L,n+1} \left(\mathbb{X}_{k,-q}^{L,n+1}\right)^{-1} \\ &= \check{\mathbf{J}}_k^{n} \check{\mathbb{X}}_{kq}^{L,n+1} \left(\mathbb{X}_{k,-q}^{L,n+1}\right)^{-1} \\ &= \underline{\mathbb{X}}_{k}^{L,n+1} \left(\mathbb{X}_{k,-q}^{L,n+1}\right)^{-1} \end{aligned} \tag{105}$$

which proves the lemma by an induction argument.

The fact that $\tilde{\underline{\mathbb{\Sigma}}}_{all_kq}^{L,n} = \underline{\mathbb{\Sigma}}_{all_k}^{L,n}$ can easily be shown using

$$\begin{aligned} \tilde{\underline{\mathbb{\Sigma}}}_{all_kq}^{L,n+1} &= \tilde{\mathbb{X}}_{kq}^{L,n+1^H} \left(\tilde{\mathbf{R}}_{all_k} + (\tau_p - 1)\tilde{\mathbf{R}}_{kq}^{B,\bar{n}}\right) \tilde{\mathbb{X}}_{kq}^{L,n+1} \\ &= \tilde{\mathbb{X}}_{kq}^{L,n+1^H} \tilde{\mathbf{J}}_k^{nH} \left(\mathbf{R}_{all_k} + (\tau_p - 1)\mathbf{R}_{kq}^{B,\bar{n}}\right) \tilde{\mathbf{J}}_k^{n} \tilde{\mathbb{X}}_{kq}^{L,n+1} \\ &= \check{\mathbb{X}}_{kq}^{L,n+1^H} \check{\mathbf{J}}_k^{nH} \left(\mathbf{R}_{all_k} + (\tau_p - 1)\mathbf{R}_{kq}^{B,\bar{n}}\right) \check{\mathbf{J}}_k^{n} \check{\mathbb{X}}_{kq}^{L,n+1} \\ &= \check{\mathbb{X}}_{kq}^{L,n+1^H} \left(\check{\mathbf{R}}_{all_k} + (\tau_p - 1)\check{\mathbf{R}}_{kq}^{B,\bar{n}}\right) \check{\mathbb{X}}_{kq}^{L,n+1} \\ &= \underline{\mathbb{\Sigma}}_{all_k}^{L,n+1}. \end{aligned} \tag{106}$$

■

Lemma B.2 partly proves Theorem IV.1. It only remains to show that $\lim_{n\to\infty} \mathbb{Q}_k^{L,n+1} = \hat{\mathbb{Q}}_k^{L}$ which can be proven as follows [50]:

$$\begin{aligned} \lim_{n\to\infty} \tilde{\mathbb{Q}}_{kq}^{L,n+1} &= \lim_{n\to\infty} \tilde{\mathbf{R}}_{\tau_k q} \tilde{\mathbb{X}}_{kq}^{L,n} \\ &= \lim_{n\to\infty} \tilde{\mathbf{J}}_{kq}^{n} \mathbf{R}_{\tau_k} \tilde{\mathbf{J}}_{kq}^{n} \tilde{\mathbb{X}}_{kq}^{L,n}. \end{aligned} \tag{107}$$

Theorem B.2 then shows that, upon convergence, $\mathbb{X}_k^L = \tilde{\mathbf{J}}_{kq}^{n} \tilde{\mathbb{X}}_{kq}^{L,n}$. (107) can thus be written as

$$\begin{aligned} \lim_{n\to\infty} \tilde{\mathbb{Q}}_{kq}^{L,n+1} &= \lim_{n\to\infty} \tilde{\mathbf{J}}_{kq}^{n} \mathbf{R}_{\tau_k} \mathbb{X}_k^L \\ &= \lim_{n\to\infty} \tilde{\mathbf{J}}_{kq}^{n} \mathbb{Q}_k^L. \end{aligned} \tag{108}$$

Selecting the first $N$ rows of (108) $\forall q$ then gives the desired result.

## ACKNOWLEDGMENT

The scientific responsibility is assumed by its authors.

## REFERENCES


[1] V. Jungnickel et al., "The role of small cells, coordinated multipoint, and massive MIMO in 5G," *IEEE Commun. Mag.*, vol. 52, no. 5, pp. 44–51, May 2014.

[2] H. Q. Ngo, A. Ashikhmin, H. Yang, E. G. Larsson, and T. L. Marzetta, "Cell-free massive MIMO: Uniformly great service for everyone," in *Proc. IEEE Workshop Signal Process. Adv. Wireless Commun.*, 2015, pp. 201–205.

[3] J. Zhang, S. Chen, Y. Lin, J. Zheng, B. Ai, and L. Hanzo, "Cell-free massive MIMO: A new next-generation paradigm," *IEEE Access*, vol. 7, pp. 99878–99888, 2019.

[4] G. Interdonato, E. Björnson, H. Q. Ngo, P. Frenger, and E. G. Larsson, "Ubiquitous cell-free massive MIMO communications," *EURASIP J. Wireless Commun. Netw.*, vol. 197, pp. 1–13, 2019.

[5] J. Kassam, D. Castanheira, A. Silva, R. Dinis, and A. Gameiro, "A review on cell-free massive MIMO systems," *Electronics*, vol. 12, no. 4, pp. 1–18, 2023.

[6] J. Zheng et al., "Mobile cell-free massive MIMO: Challenges, solutions, and future directions," *IEEE Wireless Commun.*, early access, Feb. 05, 2024, doi: 10.1109/MWC.004.2300043.

[7] A. T. Demir, E. Björnson, and L. Sanguinetti, "Foundations of user-centric cell-free massive MIMO," *Found. Trends Signal Process.*, vol. 14, no. 3/4, pp. 162–472, 2021.

[8] S. Buzzi and C. D'Andrea, "Cell-free massive MIMO: User-centric approach," *IEEE Wireless Commun. Lett.*, vol. 6, no. 6, pp. 706–709, Dec. 2017.

[9] E. Björnson and L. Sanguinetti, "Scalable cell-free massive MIMO systems," *IEEE Trans. Commun.*, vol. 68, no. 7, pp. 4247–4261, Jul. 2020.

[10] S. Chen, J. Zhang, J. Zhang, E. Björnson, and B. Ai, "A survey on user-centric cell-free massive MIMO systems," *Digit. Commun. Netw.*, vol. 8, pp. 695–719, 2022.

[11] M. Attarifar, A. Abbasfar, and A. Lozano, "Random vs structured pilot assignment in cell-free massive MIMO wireless networks," in *Proc. IEEE Int. Conf. Commun.*, 2018, pp. 1–6.

[12] S. Chen, J. J. Zhang, E. Björnson, J. J. Zhang, and B. Ai, "Structured massive access for scalable cell-free massive MIMO systems," *IEEE J. Sel. Areas Commun.*, vol. 39, no. 4, pp. 1086–1100, Apr. 2021.

[13] E. Björnson and L. Sanguinetti, "Making cell-free massive MIMO competitive with MMSE processing and centralized implementation," *IEEE Trans. Wireless Commun.*, vol. 19, no. 1, pp. 77–90, Jan. 2020.

[14] E. Björnson, L. Sanguinetti, and M. Debbah, "Massive MIMO with imperfect channel covariance information," in *Proc. IEEE 50th Asilomar Conf. Signals Syst. Comput.*, 2016, pp. 974–978.

[15] S. Haghighatshoar and G. Caire, "Massive MIMO pilot decontamination and channel interpolation via wideband sparse channel estimation," *IEEE Trans. Wireless Commun.*, vol. 16, no. 12, pp. 8316–8332, Dec. 2017.

[16] D. Neumann, M. Joham, and W. Utschick, "Covariance matrix estimation in massive MIMO," *IEEE Signal Process. Lett.*, vol. 25, no. 6, pp. 863–867, Apr. 2018.

[17] H. Xie, F. Gao, and S. Jin, "An overview of low-rank channel estimation for massive MIMO systems," *IEEE Access*, vol. 4, pp. 7313–7321, 2016.

[18] R. Van Rompaey and M. Moonen, "GEVD-based low-rank channel covariance matrix estimation and MMSE channel estimation for uplink cellular massive MIMO systems," in *Proc. IEEE 30th Eur. Signal Process. Conf.*, 2022, pp. 1641–1645.

[19] A. Özdogan, E. Björnson, and E. G. Larsson, "Massive MIMO with spatially correlated Rician fading channels," *IEEE Trans. Commun.*, vol. 67, no. 5, pp. 3234–3250, May 2019.

[20] Z. Wang, J. Zhang, E. Björnson, and B. Ai, "Uplink performance of cell-free massive MIMO over spatially correlated Rician fading channels," *IEEE Commun. Lett.*, vol. 25, no. 4, pp. 1348–1352, Apr. 2021.

[21] S. N. Jin, D. W. Yue, and H. H. Nguyen, "Spectral and energy efficiency in cell-free massive MIMO systems over correlated Rician fading," *IEEE Syst. J.*, vol. 15, no. 2, pp. 2822–2833, Jun. 2021.

[22] J. Zhang, J. Fan, B. Ai, and D. W. K. Ng, "NOMA-Based cell-free massive MIMO over spatially correlated Rician fading channels," in *Proc. IEEE Int. Conf. Commun.*, 2020, pp. 1–6.
[23] N. Shariati, E. Björnson, M. Bengtsson, and M. Debbah, "Low-complexity polynomial channel estimation in large-scale MIMO with arbitrary statistics," *IEEE J. Sel. Topics Signal Process.*, vol. 8, no. 5, pp. 815–830, Oct. 2014.
[24] A. Almamori and S. Mohan, "Estimation of channel state information (CSI) in cell-free massive MIMO based on time of arrival (ToA)," *Wireless Pers. Commun.*, vol. 114, no. 2, pp. 1825–1831, Sep. 2020.
[25] Y. Jin, J. Zhang, B. Ai, and X. Zhang, "Channel estimation for mmWave massive MIMO with convolutional blind denoising network," *IEEE Commun. Lett.*, vol. 24, no. 1, pp. 95–98, Jan. 2020.
[26] Y. Jin, J. Zhang, S. Jin, and B. Ai, "Channel estimation for cell-free mmWave massive MIMO through deep learning," *IEEE Trans. Veh. Technol.*, vol. 68, no. 10, pp. 10325–10329, Oct. 2019.
[27] E. Björnson and P. Giselsson, "Two applications of deep learning in the physical layer of communication systems [Lecture Notes]," *IEEE Signal Process. Mag.*, vol. 37, no. 5, pp. 134–140, Sep. 2020.
[28] M. Bashar, K. Cumanan, A. G. Burr, M. Debbah, and H. Q. Ngo, "On the uplink max–min SINR of cell-free massive MIMO systems," *IEEE Trans. Wireless Commun.*, vol. 18, no. 4, pp. 2021–2036, Apr. 2019.
[29] J. Zheng, J. Zhang, E. Bjornson, and B. Ai, "Impact of channel aging on cell-free massive MIMO over spatially correlated channels," *IEEE Trans. Wireless Commun.*, vol. 20, no. 10, pp. 6451–6466, Oct. 2021.
[30] H. Q. Ngo, A. Ashikhmin, H. Yang, E. G. Larsson, and T. L. Marzetta, "Cell-free massive MIMO versus small cells," *IEEE Trans. Wireless Commun.*, vol. 16, no. 3, pp. 1834–1850, Mar. 2017.
[31] G. Interdonato, M. Karlsson, E. Björnson, and E. G. Larsson, "Local partial zero-forcing precoding for cell-free massive MIMO," *IEEE Trans. Wireless Commun.*, vol. 19, no. 7, pp. 4758–4774, Jul. 2020.
[32] J. Zhang, J. Zhang, E. Björnson, and B. Ai, "Local partial zero-forcing combining for cell-free massive MIMO systems," *IEEE Trans. Commun.*, vol. 69, no. 12, pp. 8459–8473, Dec. 2021.
[33] D. Maryopi, M. Bashar, and A. G. Burr, "On the uplink throughput of zero forcing in cell-free massive MIMO with coarse quantization," *IEEE Trans. Veh. Technol.*, vol. 68, no. 7, pp. 7220–7224, Jul. 2019.
[34] X. Wang, J. Cheng, C. Zhai, and A. Ashikhmin, "Partial cooperative zero-forcing decoding for uplink cell-free massive MIMO," *IEEE Internet Things J.*, vol. 9, no. 12, pp. 10327–10339, Jun. 2022.
[35] J. Zhang, J. Zhang, D. W. K. Ng, S. Jin, and B. Ai, "Improving sum-rate of cell-free massive MIMO with expanded compute-and-forward," *IEEE Trans. Signal Process.*, vol. 70, pp. 202–215, 2022.
[36] A. Bertrand and M. Moonen, "Distributed adaptive node-specific signal estimation in fully connected sensor networks–Part I: Sequential node updating," *IEEE Trans. Signal Process.*, vol. 58, no. 10, pp. 5277–5291, Oct. 2010.
[37] J. Szurley, A. Bertrand, and M. Moonen, "Topology-independent distributed adaptive node-specific signal estimation in wireless sensor networks," *IEEE Trans. Signal Inf. Process. Netw.*, vol. 3, no. 1, pp. 130–144, Mar. 2017.
[38] A. Hassani, A. Bertrand, and M. Moonen, "GEVD-Based low-rank approximation for distributed adaptive node-specific signal estimation in wireless sensor networks," *IEEE Trans. Signal Process.*, vol. 64, no. 10, pp. 2557–2572, May 2016.
[39] R. Van Rompaey and M. Moonen, "Distributed adaptive node-specific signal estimation in a wireless sensor network with partial prior knowledge of the desired source steering matrix," *IEEE Trans. Signal Inf. Process. Netw.*, vol. 7, pp. 478–492, Jul. 2021.
[40] T. L. Marzetta and H. Q. Ngo, *Fundamentals of Massive MIMO*. Cambridge, U.K.: Cambridge Univ. Press, 2016.
[41] E. Björnson, J. Hoydis, and L. Sanguinetti, "Massive MIMO networks: Spectral, energy, and hardware efficiency," *Found. Trends Signal Process.*, vol. 11, no. 3/4, pp. 154–655, 2017.
[42] R. Serizel, M. Moonen, B. Van Dijk, and J. Wouters, "Low-rank approximation based multichannel wiener filter algorithms for noise reduction with application in cochlear implants," *IEEE/ACM Trans. Audio Speech Lang. Process.*, vol. 22, no. 4, pp. 785–799, Apr. 2014.
[43] R. Van Rompaey and M. Moonen, "Scalable and distributed MMSE algorithms for uplink receive combining in cell-free massive MIMO systems," in *Proc. IEEE Int. Conf. Acoust. Speech Signal Process.*, 2021, pp. 4445–4449.
[44] R. Van Rompaey and M. Moonen, "Distributed MMSE–based uplink receive combining, downlink transmit precoding and optimal power allocation in cell–free massive MIMO systems," *EURASIP J. Wireless Commun. Netw.*, vol. 2023, 2023, Art. no. 48.
[45] A. Dimakis, S. Kar, J. Moura, M. G. Rabbat, and A. Scaglione, "Gossip algorithms for distributed signal processing," *Proc. IEEE*, vol. 98, no. 11, pp. 1847–1864, Nov. 2010.
[46] Y. Zeng and R. C. Hendriks, "Distributed delay and sum beamformer for speech enhancement via randomized gossip," *IEEE Trans. Audio Speech Lang. Process.*, vol. 22, no. 1, pp. 260–273, Jan. 2014.
[47] A. Bertrand and M. Moonen, "Distributed adaptive generalized eigenvector estimation of a sensor signal covariance matrix pair in a fully connected sensor network," *Signal Process.*, vol. 106, pp. 209–214, Jan. 2015.
[48] H. Chen, A. Campbell, B. Thomas, and A. Tamir, "Minimax flow tree problems," *Networks*, vol. 54, pp. 117–129, 2009.
[49] Z. Wang, J. Zhang, B. Ai, C. Yuen, and M. Debbah, "Uplink performance of cell-free massive MIMO with multi-antenna users over jointly-correlated rayleigh fading channels," *IEEE Trans. Wireless Commun.*, vol. 21, no. 9, pp. 7391–7406, Sep. 2022.
[50] A. Hassani, A. Bertrand, and M. Moonen, "Distributed signal subspace estimation based on local generalized eigenvector matrix inversion," in *Proc. 23rd Eur. Signal Process. Conf.*, 2015, pp. 1386–1390.

**ROBBE VAN ROMPAEY** (Member, IEEE) was born in Bonheiden, Belgium, in 1994. He received the M.Sc. degree (*magna cum laude*) in electrical engineering and the Ph.D. degree under the supervision of Prof. M. Moonen from the Electrical Engineering Department, KU Leuven, Leuven, Belgium, in 2017, and 2022, respectively. His research interests include multi-channel signal processing, wireless sensor networks, distributed optimization and distributed signal processing with application in speech/audio processing, and MIMO communications. He is a Fellow of the Research Foundation—Flanders and is currently involved in a joint project with KU Leuven and Nokia Bell Labs, Antwerp, Belgium.

**MARC MOONEN** (Fellow, IEEE) is a Full Professor with the Electrical Engineering Department, KU Leuven, Leuven, Belgium, where he is heading a research team working in the area of numerical algorithms and signal processing for digital communications, wireless communications, DSL, and audio signal processing. He is a Fellow of EURASIP (2018). He received the 1994 KU Leuven Research Council Award, the 1997 Alcatel Bell (Belgium) Award (with Piet Van- daele), and the 2004 Alcatel Bell (Belgium) Award (with Raphael Cendrillon), and was a 1997 Laureate of the Belgium Royal Academy of Science. He received journal best paper awards from the IEEE TRANSACTIONS ON SIGNAL PROCESSING (with Geert Leus and with Daniele Giacobello) and *Elsevier Signal Processing* (with Simon Doclo). He was Chairman of the IEEE Benelux Signal Processing Chapter during 1998–2002, a Member of the IEEE Signal Processing Society Technical Committee on Signal Processing for Communications, and President of EURASIP (European Association for Signal Processing, 2007–2008 and 2011–2012). He was the Vice-President for Publications of the IEEE Signal Processing Society (2021–2023). He was the Editor-in-Chief of *EURASIP Journal on Applied Signal Processing* during 2003–2005, Area Editor for Feature Articles in *IEEE Signal Processing Magazine* during 2012–2014, and has been a Member of the editorial board of *Signal Processing*, IEEE TRANSACTIONS ON CIRCUITS AND SYSTEMS II, *IEEE Signal Processing Magazine*, *Integration-the VLSI Journal*, *EURASIP Journal on Wireless Communications and Networking*, and *EURASIP Journal on Advances in Signal Processing*.